

Viscosity Reduction of Paraffinic Crude Using Pulsated Magnetic Field

A Report Submitted by

Deepak Pandey (R820211011) & Samyak Suyal (R820211030)

*in partial fulfillment of the requirements
for the award of the degree of*

BACHELOR OF TECHNOLOGY
In
APPLIED PETROLEUM ENGINEERING
with specialization in
GAS ENGINEERING

Under the Guidance of
Mr. R. P. Soni



**DEPARTMENT OF CHEMICAL ENGINEERING
COLLEGE OF ENGINEERING STUDIES**

University of Petroleum & Energy Studies

Bidholi Campus, Energy Acres,
Dehradun - 248007

April - 2015

Certificate of Approval

It is to certify that the project entitled, “*Viscosity Reduction of Paraffinic Crude Using Pulsated Magnetic Field*” was submitted by **Mr. Deepak Pandey (R820211011) & Samyak Suyal (R820211030)**, to the University of Petroleum & Energy Studies, for the award of degree of **BACHELOR OF TECHNOLOGY in Applied Petroleum Engineering** with specialization in **Gas Engineering** is a bonafide record of project work carried out by them under my supervision.

The same is hereby approved.



Mr. R. P. Soni
Prof. Production Engineering
Department of Petroleum Engineering & Earth Sciences
University of Petroleum & Energy Studies

Acknowledgement

At the outset, it is our duty to express our deep sense of gratitude to **Dr. Kamal Bansal, Dean (COES)** and to **Dr Ashutosh Pandey, HOD (Chemical Dept)** for extending the opportunity for undergoing Dissertation project, and providing all the necessary resources and expertise for this purpose.

We are thankful to **Mr. R P Soni** for his encouragement and cooperation. He took painstaking effort in order to make our project a fruitful learning experience by supporting us at all points. We are also grateful to **Mr. B Shingan, Course Co-ordinator (B. Tech APE-Gas)** for his constant support throughout the project. The resources and laboratories of the University of Petroleum & Energy Studies have been of constant help in our process of making this project. We are grateful to all our friends and colleagues for their funding and co-operation in the accumulation of information and material for the successful completion of the Project.

Also we would express our deep sense of gratitude to **Mr. M. S. Jatawat (DGM ONGC)** and **Mr. T. N. More (Chief Engineer ONGC)** for providing us the crude and share their valuable time and support.

Last but not the least, we would thank **Mr. Abhishek Attri (Lab. Attendant, Nanotechnology Lab)**, **Mr. Mukesh (Lab. Attendant, Physics Lab)**, and **Mr. Vishal Bhandari (Lab. Attendant, Petroleum Testing Lab)** for assisting us in many ways.

THE NATION BUILDERS UNIVERSITY

Table of Contents

Certificate of Approval	2
Acknowledgement	3
List of Figures	7
List of Tables	10
Annexure Contents.....	12
Project Summary.....	13
Abstract.....	14
Chapter 1: Literature Survey.....	15
1.1. Introduction	15
1.2. Thermal Insulation and Pipeline Heating.....	15
1.3. Inhibitor Injection Method	16
1.3.1. Thermodynamic Wax Inhibitor (TWI)	16
1.3.2. Pour Point Depressants	17
1.3.3. Crystal Modifiers	19
1.3.4. Surfactants / Dispersants.....	20
1.4. Transportation below Pour Point	20
1.5. Viscosity Reduction by Permanent Magnets – Case Study of Nigerian Crude	21
1.6. Effect of Magnetic Field on Less Paraffinic crude - Case Study of American Crude ...	22
1.7. Viscosity Reduction using an Electromagnet – New Concept.....	24
1.7.1. Advantage over Permanents Magnets.....	25
1.8. Modified Scheme for Pilot Experiment using an Electromagnet.....	25
Chapter 2: Static Experimental Run	26
2.1. Design of Experimental Setup for Static Run	26
2.1.1. Theoretical Design of Apparatus 1	26
2.1.2. Failure of Apparatus 1	27
2.1.3. Technical Outcomes from the Failures and Theoretical Design of Apparatus 2	28
2.1.4. Limitation of Hall Effect Magnetic Field Sensor and Uncertainty in Apparatus 2	30

2.1.5.	Apparatus 3 for Static Test	31
2.2.	Procedure for Static Test	31
Chapter 3: Observations & Outcomes from Static Experiment.....		33
3.1.	Viscometer Calibration	33
3.1.1.	Interpolation of Laboratory's Data at 46° C Temperature.....	33
3.2.	Readings at 7500 Gauss Magnetic Field	34
3.2.1.	Initial Reading.....	34
3.2.2.	Second Reading	35
3.2.3.	Third Reading	35
3.2.4.	Conclusion from Magnetic Treating at 7500 Gauss	36
3.3.	Readings at 6800 Gauss	37
3.3.1.	Initial Reading.....	37
3.3.2.	Second Reading	38
3.3.3.	Third Reading	38
3.3.4.	Conclusion from Magnetic Treating at 6800 Gauss	39
3.4.	Readings at 6500 Gauss	43
3.4.1.	Initial Reading.....	43
3.4.2.	Second Reading	43
3.4.3.	Third Reading	44
3.4.4.	Conclusion from Magnetic Treating at 6500 Gauss	44
3.5.	Readings at 8000 and 9000 Gauss.....	47
3.6.	Conclusion from the Static Experiment	47
3.7.	Viscosity Regain Time Test	48
3.7.1.	Viscosity Regain Test for 7 hours.....	48
3.7.2.	Viscosity Regain Test for 8 hours.....	51
Chapter 4: Dynamic Experimental Run.....		54
4.1.	Design of Experimental Setup for Dynamic Run.....	54
4.1.1.	Theoretical Design of Apparatus 1	54
4.1.2.	Failure of Apparatus 1 and Rectification of its Limitation	55

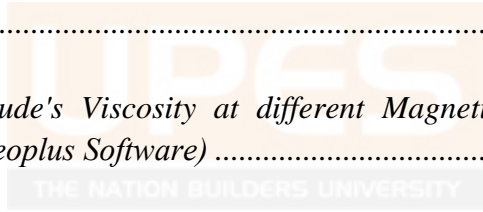
4.1.3. Apparatus 2 for Dynamic Test.....	56
4.2. Procedure of Dynamic Test.....	57
 Chapter 5: Observations & Outcomes from Dynamic Experiment	58
5.1. Apparatus Calibration	58
5.1.1. Calculation for Desired Flow Rate	58
5.1.2. Temperature Control.....	59
5.2. Readings at 6500 Gauss Magnetic Field.....	59
5.2.1. Initial Reading.....	59
5.2.2. Second Reading	60
5.2.3. Third Reading	60
5.2.4. Conclusion from Magnetic Treating at 6500 Gauss	61
 Conclusion & Recommendation.....	65
6.1. Static Experiment Constraints.....	65
6.2. Dynamic Experiment Constraints	66
6.3. Laboratory Constraints.....	66
6.4. Recommendation for future development.....	66
 References.....	68
 Annexure.....	69

List of Figures

<i>Figure 1: The 9000 kW system used to heat 43 km long subsea production pipeline between Lianzi Field and Benguela Belize Lobitio Tomboco (BBLT) (Source: www.techrelease.com)....</i>	16
<i>Figure 3: Molecular Structure of Typical Pour Point Depressants</i>	17
<i>Figure 4: A too High Molecular Weight Polymer may Entangle Itself Instead of Interacting with Paraffins (left), and A to Low Molecular Weight Polymer may not have a sufficient Molecular Volume to Disrupt Paraffin Crystallization (right)</i>	18
<i>Figure 5: PPD Inhibition Mechanism of Wax Modification – Chemical Structure of Wax (2A); Crystal Shape of Wax Structure (2B); Crystal Structure of Growing Wax Lattice (2C); Polymeric Additive with Wax – like Components (2D); Co – crystallization of Wax and PPD (2E); and Stirically Hindered Wax Structure (2F)</i>	18
<i>Figure 6: Prevention Mechanism of Interlocking Wax Crystals by Polymer Additive – Nucleating Site interaction (red) to Asphaltene & Wax Molecules (blue) (1st Figure); Polar Component of Additive (green) Hinder Co – crystallization of Asphaltenes & Wax (2nd Figure)</i>	19
<i>Figure 7: Structure of Surfactant.....</i>	20
<i>Figure 8: Niger Delta Region, Nigeria.....</i>	21
<i>Figure 9: Carbon Number Distribution in Wax</i>	22
<i>Figure 10: Brookfield Viscometer, UL adapter with a precision cylindrical spindle rotating inside.....</i>	23
<i>Figure 11: Viscosity – time curve of paraffin based crude oil sample at 10° C and 10 RPM was down to 33.1 CP from 40.97 CP after applying the magnetic field of 1.33 Tesla for 50 seconds (Source: Energy & Fuels 2006, 20).....</i>	23
<i>Figure 12: Theoretical Design of Apparatus 1.....</i>	26
<i>Figure 13: Structure of Apparatus 1.....</i>	27
<i>Figure 14: Theoretical Design of Apparatus 2.....</i>	29
<i>Figure 15: Structure of Apparatus 2.....</i>	29

<i>Figure 16: Limitation of Hall Effect Sensor in Sensing Magnetic Field at the Center</i>	<i>30</i>
<i>Figure 17: Hall Effect Equipment and Accessories (684 x10 Gauss reading at 2.86 Ampere Current with 1.25 Inch Air Gap Between the two poles of Electromagnet)</i>	<i>31</i>
<i>Figure 18: Viscosity Details of Crude at Different Temperatures</i>	<i>33</i>
<i>Figure 19: Comparison of Viscosity before treating and after treating at 7500 Gauss Magnetic Field</i>	<i>36</i>
<i>Figure 20: Comparison of Viscosity before treating and after treating at 6800 Gauss Magnetic Field</i>	<i>39</i>
<i>Figure 21: Behavior of Relaxation Modulus of Crude after treating in Magnetic Field of 6800 Gauss.....</i>	<i>40</i>
<i>Figure 22: Behavior of Deflection Angle of Crude after treating in Magnetic Field of 6800 Gauss.....</i>	<i>42</i>
<i>Figure 23: Comparison of Viscosity before treating and after treating at 6500 Gauss Magnetic Field</i>	<i>45</i>
<i>Figure 24: Behavior of Relaxation Modulus of Crude after treating in Magnetic Field of 6500 Gauss.....</i>	<i>46</i>
<i>Figure 25: Behavior of Deflection Angle of Crude after treating in Magnetic Field of 6500 Gauss.....</i>	<i>47</i>
<i>Figure 26: Behavior of Crude's Viscosity at different Magnetic Field Intensity (Courtesy: Snapshot of Anton Parr's Rheoplus Software)</i>	<i>48</i>
<i>Figure 27: Behavior of Viscosity after 7 hours at 6500 Gauss Magnetic Field.....</i>	<i>49</i>
<i>Figure 28: Behavior of Relaxation Modulus after 7 hours at 6500 Gauss Magnetic Field.....</i>	<i>49</i>
<i>Figure 29: Behavior of Deflection Angle after 7 hours at 6500 Gauss Magnetic Field</i>	<i>51</i>
<i>Figure 30: Behavior of Viscosity after 8 hours at 6500 Gauss Magnetic Field.....</i>	<i>51</i>
<i>Figure 31: Behavior of Relaxation Modulus after 8 hours at 6500 Gauss Magnetic Field.....</i>	<i>53</i>

<i>Figure 32: Behavior of Deflection Angle after 8 hours at 6500 Gauss Magnetic Field</i>	<i>53</i>
<i>Figure 33: Theoretical Design of Apparatus 1 for Dynamic Run</i>	<i>54</i>
<i>Figure 34: Fabricated Apparatus 1 for Dynamic Run</i>	<i>55</i>
<i>Figure 35: Theoretical Design of Apparatus 2.....</i>	<i>56</i>
<i>Figure 36: Apparatus 2.....</i>	<i>56</i>
<i>Figure 37: Comparison of Viscosity before treating and after treating at 6500 Gauss Magnetic Field</i>	<i>61</i>
<i>Figure 38: Behavior of Relaxation Modulus of Crude after treating in Magnetic Field of 6500 Gauss.....</i>	<i>62</i>
<i>Figure 39: Behavior of Deflection Angle of Crude after treating in Magnetic Field of 6500 Gauss.....</i>	<i>63</i>
<i>Figure 40: Behavior of Crude's Viscosity at different Magnetic Field Intensity (Courtesy: Snapshot of Anton Parr's Rheoplus Software)</i>	<i>64</i>



List of Tables

<i>Table 1: Reading 1 at 7500 Gauss</i>	34
<i>Table 2: Reading 2 at 7500 Gauss</i>	35
<i>Table 3: Reading 3 at 7500 Gauss</i>	35
<i>Table 4: Compiled Reading at 7500 Gauss</i>	36
<i>Table 5: Reading 1 at 6800 Gauss</i>	37
<i>Table 6: Reading 2 at 6800 Gauss</i>	38
<i>Table 7: Reading 3 at 6800 Gauss</i>	38
<i>Table 8: Compiled Reading at 6800 Gauss</i>	39
<i>Table 9: Compiled Relaxation Modulus Data at 6800 Gauss Magnetic Field</i>	40
<i>Table 10: Compiled Deflection Angle Data at 6800 Gauss Magnetic Field</i>	41
<i>Table 11: Reading 1 at 6500 Gauss Magnetic Field</i>	43
<i>Table 12: Reading 2 at 6500 Gauss</i>	43
<i>Table 13: Reading 3 at 6500 Gauss</i>	44
<i>Table 14: Compiled Reading at 6500 Gauss</i>	44
<i>Table 15: Compiled Relaxation Modulus Data at 6500 Gauss Magnetic Field</i>	45
<i>Table 16: Compiled Deflection Angle Data at 6500 Gauss Magnetic Field</i>	46
<i>Table 17: Details of 6 hours 40 minutes Viscosity Regain Test</i>	50
<i>Table 18: Details of 7 hours 50 minutes Viscosity Regain Test</i>	53
<i>Table 19: Reading 1 at 6500 Gauss</i>	59

Table 20: Reading 2 at 6500 Gauss..... 60

Table 21: Reading 3 at 6500 Gauss..... 60

Table 22: Compiled Reading at 6500 Gauss 61

Table 23: Compiled Relaxation Modulus Data at 6500 Gauss Magnetic Field..... 62

Table 24: Compiled Deflection Angle Data at 6500 Gauss Magnetic Field..... 63



Annexure Contents

<i>Snapshot 1: Reading 1 at 6800 Gauss Magnetic Field.....</i>	<i>69</i>
<i>Snapshot 2: Reading 2 at 6800 Gauss Magnetic Field.....</i>	<i>70</i>
<i>Snapshot 3: Reading 3 at 6800 Gauss Magnetic Field.....</i>	<i>71</i>
<i>Snapshot 4: Reading 1 6500 Gauss</i>	<i>72</i>
<i>Snapshot 5: Reading 2 at 6500 Gauss Magnetic Field.....</i>	<i>73</i>
<i>Snapshot 6: Reading 3 at 6500 Gauss Magnetic Field.....</i>	<i>74</i>
<i>Snapshot 7: Compiled Static Readings</i>	<i>75</i>
<i>Snapshot 8: Compiled Dynamic Reading</i>	<i>75</i>



Project Summary

Aim of Project– To reduce the viscosity of Paraffinic crude by the means of Pulsed Magnetic field generated from Electromagnet.

Place of Experiment – Nanotechnology Lab and Physics Lab

Equipment Used – AntonParr Rheometer, Hall Effect Apparatus, Florescence Microscope, Hot Air Oven, Gauss meter.

Software Used - Rheoplus

Crude Category – Paraffinic in nature (24 – 27 % paraffin content by wt.)

Lab Project Cost Estimates – 15000 INR approx.

Project Schedule – First Phase

Objective	Month
Literature Survey I – Conventional Methods (Pipeline Heating, Inhibitor Injection & Below Pour Point Transportation)	September – October
Literature Survey II – Magnetic Methods (Using Permanent Methods & Electro Magnets)	November
Experimental Setup Design for Static Run	December

Second Phase

Objective	Month
Static Experiment Execution & Design for Dynamic Run	January
Dynamic Experiment Run	February
Calculations & Suggestions	March
Final Project Review	April

Abstract

The project aims at scaling down the viscosity of paraffinic crude by subjecting it under magnetic field for short continuance. This experimentation is an annex of the proposal made in order to correct the limitations of Rongjia Tao, who performed the experiment on less viscous paraffinic crude under laboratory constraints. The experiment consists of two stages i.e. static and dynamic run. In static run the validity of Tao's experimental results is tested in a viscometer and an efficient value of magnetic field is determined for the particular crude oil. Once the validity of magnetic field effect on paraffinic crude has been established, then the experiment is performed on dynamic run where the crude oil is magnetized inside the piping systems under the flowing conditions. If the viscosity-time curve from static and dynamic conditions follows the same trend in the viscometer then it can be conducted for the pilot experiment in the pipelines.

Keywords: viscosity, magnetic field, viscometer, pipeline, paraffinic, crude oil, laboratory constrains, dynamic.



Chapter 1: Literature Survey

1.1. Introduction

The viscosity of a fluid is a measure of resistance to the gradual deformation by shear stress. It arises from the friction between the neighboring particles in fluid that are moving with different velocities. For example, when the fluid is allowed to move in the tube, then the particles which comprise the fluid generally move faster near the tube axis and slower in the walls. Therefore, the resistance offered by the different adjacent layers of fluid to oppose the flow is termed as viscosity.

Viscosity is one of the important key properties of the crude oil and it varies from 10 cP to 100,000 cP depending upon the composition of crude (Paraffin based, Asphalt based or Mix based). In crude oils, Paraffin precipitation increases the system apparent viscosity promoting loss of fluidity, depending on the operating temperature. This results in the deposition of paraffin inside the tubing which leads to choking and causes difficulty in the flow of crude through the pipelines. Apart from crude composition and temperature, pressure and particle agglomeration also affects the viscosity of paraffinic crude.

Therefore, different methods have been adopted in order to reduce the viscosity of paraffinic crude and provide ease in the transportation. These methods include blending the crude with the polymers which stabilizes the wax content and preventing it to agglomerate or using the heat treatment to reduce the viscosity of crude. Recently, a team of researchers under Rongjia Tao, a physicist at Temple University in Philadelphia, had found that a strong magnetic field can also reduce the viscosity of paraffin based crude.

Some commonly used methods have been discussed in this literature survey.

1.2. Thermal Insulation and Pipeline Heating

The viscosity of crude is inversely proportional to the temperature. It is because of the fact, that on increasing the temperature, the paraffin particles attain the heat energy which imparts kinetic energy to the particles. Due to this, the wax particles tend to disintegrate into the smaller particles from their larger clusters which in turn decreases the resistance offered by the adjacent layers to the flow and finally lowers the crude's viscosity.

Using the same concept, the viscosity of crude is reduced within the pipeline. A section of pipeline (or sometimes a whole pipeline) is wrapped with the coil through which it is to be heated followed by the insulation to prevent the lowering of temperature within the pipeline. A good thermal insulation can keep the fluid above the cloud point of the whole flow-line and therefore eliminate wax deposition. Sometimes hot fluid is also mixed with the crude to reduce the apparent viscosity. Removal of wax by the means of hot fluid or electric heating works well for down-hole and for short flow-lines.



Figure 1: The 9000 kW system used to heat 43 km long subsea production pipeline between Lianzi Field and Benguela Belize Lobitio Tomboco (BBLT) (Source: www.techrelease.com)

Continuously heating the pipeline section over a large distance is quite energy exhaustive. It has been found that about 1.32 Quadrillion Btu amount of energy has been used to heat the pipeline every year. Moreover, injecting the hot polymer into the crude not only degrade the quality of crude but also proves to be much more costly. Also, the separation of injected polymers would lead to environmental damage also.

1.3. Inhibitor Injection Method

Chemical inhibitors can also reduce the deposition rates of waxy crude. The commonly used chemical inhibitors types for wax prevention include:

1. Thermodynamic Wax Inhibitor (TWI)
2. Pour Point Depressants
3. Crystal Modifiers
4. Surfactants / Dispersants

1.3.1. Thermodynamic Wax Inhibitor (TWI)

These inhibitors suppress the cloud point, pour point and viscosity of crude by changing the crude's thermodynamic properties. Parachek® 160™ inhibitor (by Halliburton) and other chlorinated paraffin complexes have been made in order to prevent the wax appearance inside the tubing. But these chemicals are injected in large proportions.

1.3.2. Pour Point Depressants

These substances modify the structure of wax crystals such that it could not form larger agglomerates. This leads to decrease in the yield stress between the adjacent layers of the molecules and thus reduces the viscosity of crude. Moreover, they are also used to reduce the pour point of crude so that the crude could flow even in the cold temperature zones. But these depressants cannot reduce the rate of wax deposition.

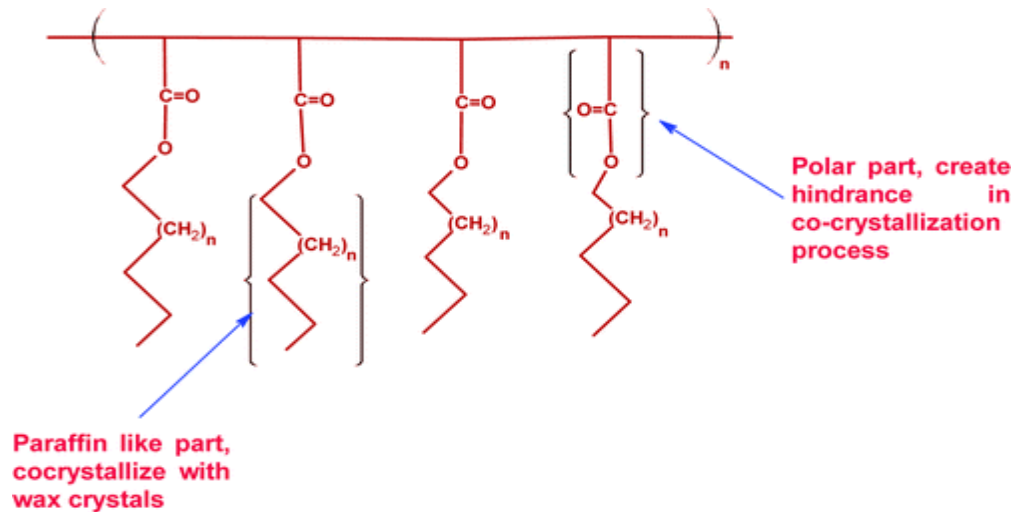


Figure 2: Molecular Structure of Typical Pour Point Depressants

Pour-point depressants (PPDs) are designed to be cost-effective methods to improve cold-flow properties of crude and other fuel oils to remain primarily as a fluid. PPDs typically have three components:

1. A wax-like paraffinic part composed primarily of linear alkyl chains of 14 to 25 carbon atoms long, which co-crystallizes with the oil's wax-forming components
2. A polar component to limit the degree of co-crystallization.
3. A primary component composed of polymers which, when attached to the wax crystal, will sterically hinder growth of large crystals.

Generally, the polar component of the additive creates the barrier to the formation of the interlocking crystal wax network. As a result, the altered shape and smaller size of the wax crystals reduce the formation of the interlocking networks and reduces the pour point.

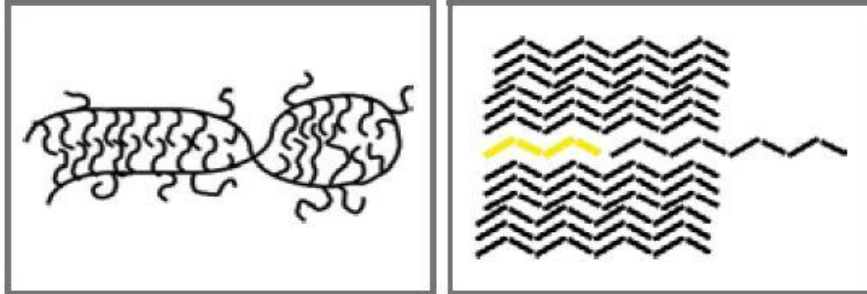


Figure 3: A too High Molecular Weight Polymer may Entangle Itself Instead of Interacting with Paraffins (left), and A to Low Molecular Weight Polymer may not have a sufficient Molecular Volume to Disrupt Paraffin Crystallization (right)

Working Mechanism of Pour Point Depressants (PPDs)

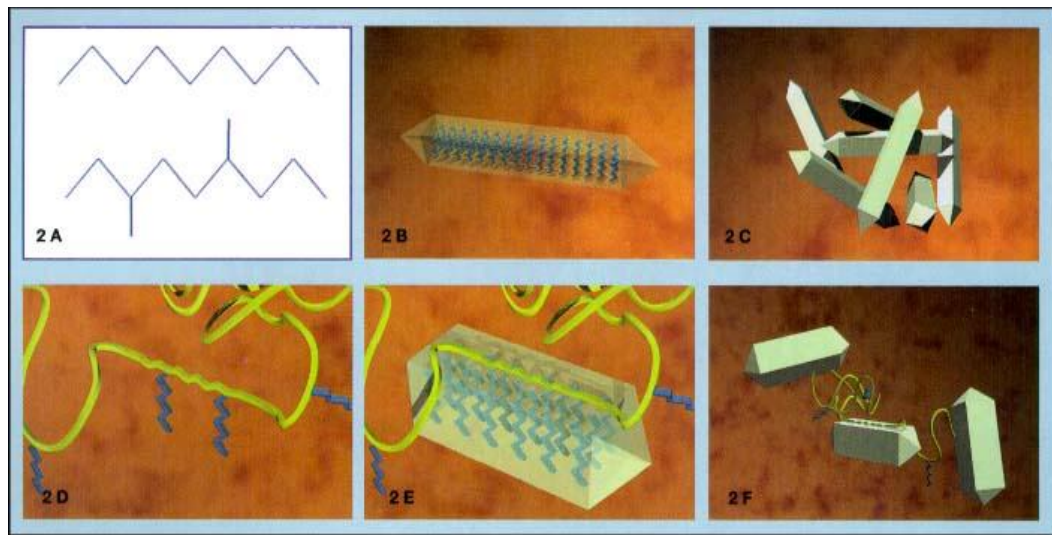


Figure 4: PPD Inhibition Mechanism of Wax Modification – Chemical Structure of Wax (2A); Crystal Shape of Wax Structure (2B); Crystal Structure of Growing Wax Lattice (2C); Polymeric Additive with Wax – like Components (2D); Co – crystallization of Wax and PPD (2E); and Sterically Hindered Wax Structure (2F)

The mechanism to prevent agglomeration primarily involves the structure of the PPDs to disrupt the crystal habit of wax crystals. Structures involved in this process are: the pendant chains to co-crystallize with the wax and the polar end groups which are responsible for disrupting the orthorhombic crystal structure into a compact pyramidal form. This process prevents the crystals from agglomerating and forming a gel-like structure to deposit on the pipeline surface.

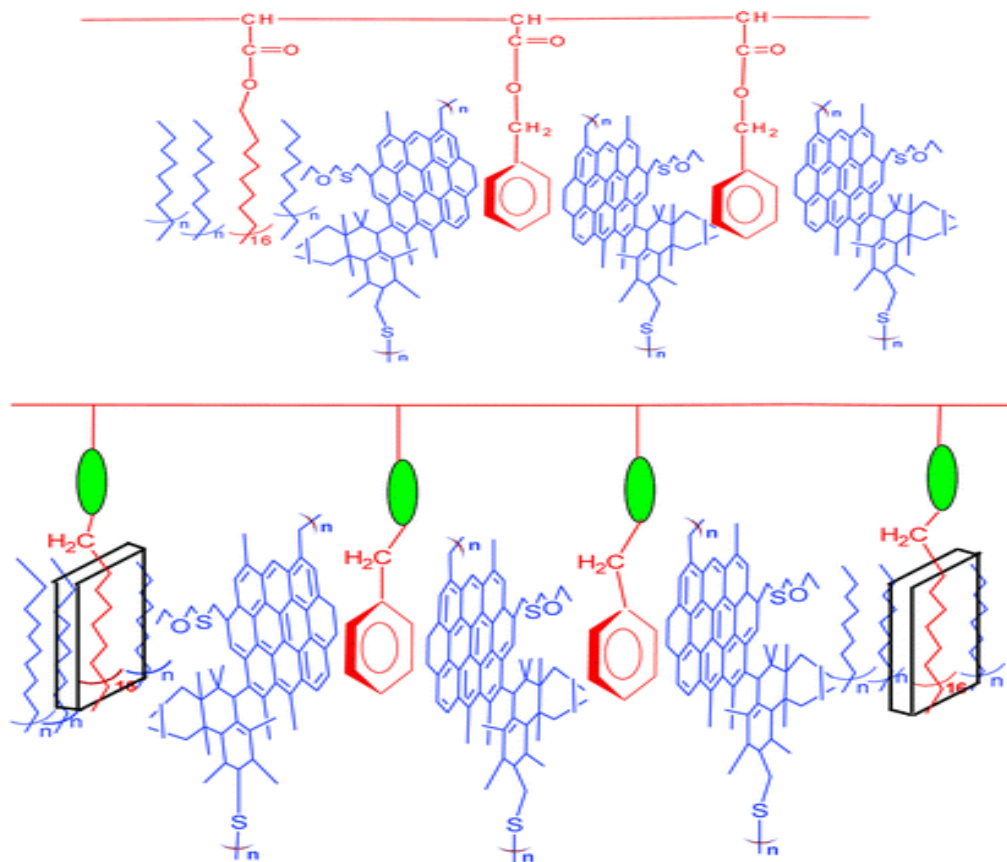


Figure 5: Prevention Mechanism of Interlocking Wax Crystals by Polymer Additive – Nucleating Site interaction (red) to Asphaltene & Wax Molecules (blue) (1st Figure); Polar Component of Additive (green) Hinder Co – crystallization of Asphaltenes & Wax (2nd Figure)

The efficacy of the additive generally depends on the rheological properties on the crude oil. As such, the crude containing comparable amount of asphaltenes may not react in the same manner as paraffin predominate crudes. Asphaltenes in crude behave as a natural PPD, and can hinder the growth of wax crystals by attaching to the surface of the wax crystals. So, incorporating an additive into the crude can diminish the interaction between the additive and the wax crystals resulting in a poor performance of the PPD. A single PPD cannot effectively depress the pour point of all types of crudes. Specifically tailored PPDs must be designed to match the crude's paraffin chain length and composition to participate efficiently in the crystallization of wax crystals to depress the pour point.

1.3.3. Crystal Modifiers

These substances co-crystallize the wax structures in order to weaken the adhesion and prevent the wax formation in pipes. Once the wettability particles have been changed, these wax particles could no longer merge to form larger clusters and hence the surface tension between them has been reduced. Once the surface tension has been reduced, then, the friction requires to overcome the flow is reduced and the viscosity is lowered. These

substances are very costly and need to be injected at higher pressure and above the cloud point of crude.

1.3.4. Surfactants / Dispersants

Surfactants are employed in pipelines to discourage the formation of paraffins in favorable amounts. The use of surfactants is an accepted method for dealing with flow problems caused by paraffins and asphaltene fouling and is often employed in drilling operations as well.

Working Mechanism of Surfactants

The general surfactant includes the following components:

1. Hydrophilic section ("water-loving")
2. Hydrophobic section (repelled by water), which may also be lipophilic (dissolves in oils and non-polar solvents)

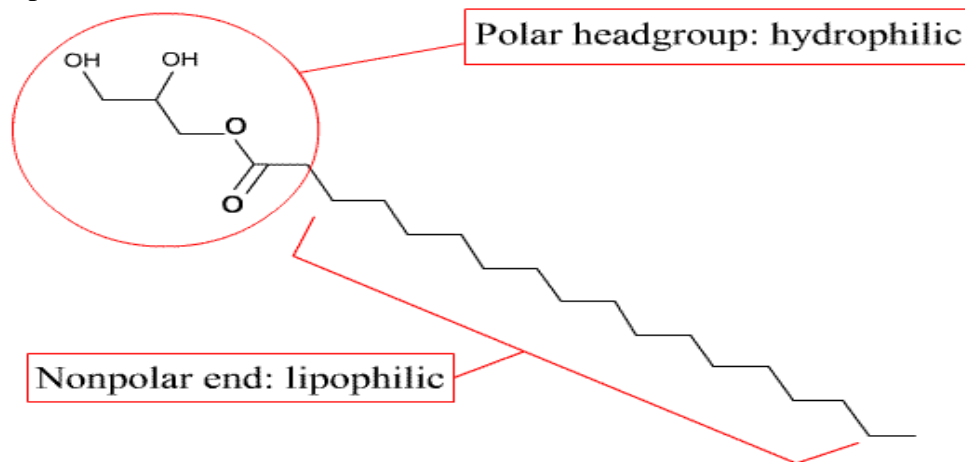


Figure 6: Structure of Surfactant

These two parts of the surfactant molecule act in concert to encapsulate paraffin droplets (in the case of usage in pipelines) and keep them emulsified in the product stream. This trapping of small clusters of paraffin is achieved by the strong dipole-dipole interaction between the hydrophilic (polar) end of the surfactant molecule and any water in the product stream. The surfactant molecule is oriented by these forces such that it forms a barrier between any paraffin and any water in the product stream, which inhibits the accumulation of paraffin in the pipeline.

1.4. Transportation below Pour Point

This method is used for short distance pipelines up to 50 km. In this method, the temperature of crude is first lowered below its pour point and then pumped into pipelines by the means of high pressure reciprocating pumps. Due to the sudden jerk applied by high pressure, there is a breakdown of larger paraffin particles into smaller ones which in turn reduces the viscosity

of crude. But the main thing which is taken into the account is that the pressure should be constant throughout the pipeline.

1.5. Viscosity Reduction by Permanent Magnets – Case Study of Nigerian Crude

Nigeria is the largest oil producer in Africa and the eleventh largest in the world. ChevronTexaco, ExxonMobil, Total, Agip, and ConocoPhillips are the major multinationals involved in the Nigeria oil sector. The main production activity in Nigeria is in the Niger Delta region, which according to the master plan, extends over an area of about 70,000 square kilometers which amounts 7.5% of Nigeria's land mass. The Niger Delta is a world's third largest wetland after Holland and Mississippi. It covers a coastline of 560 km, which is about two-thirds of the entire coastline of Nigeria.

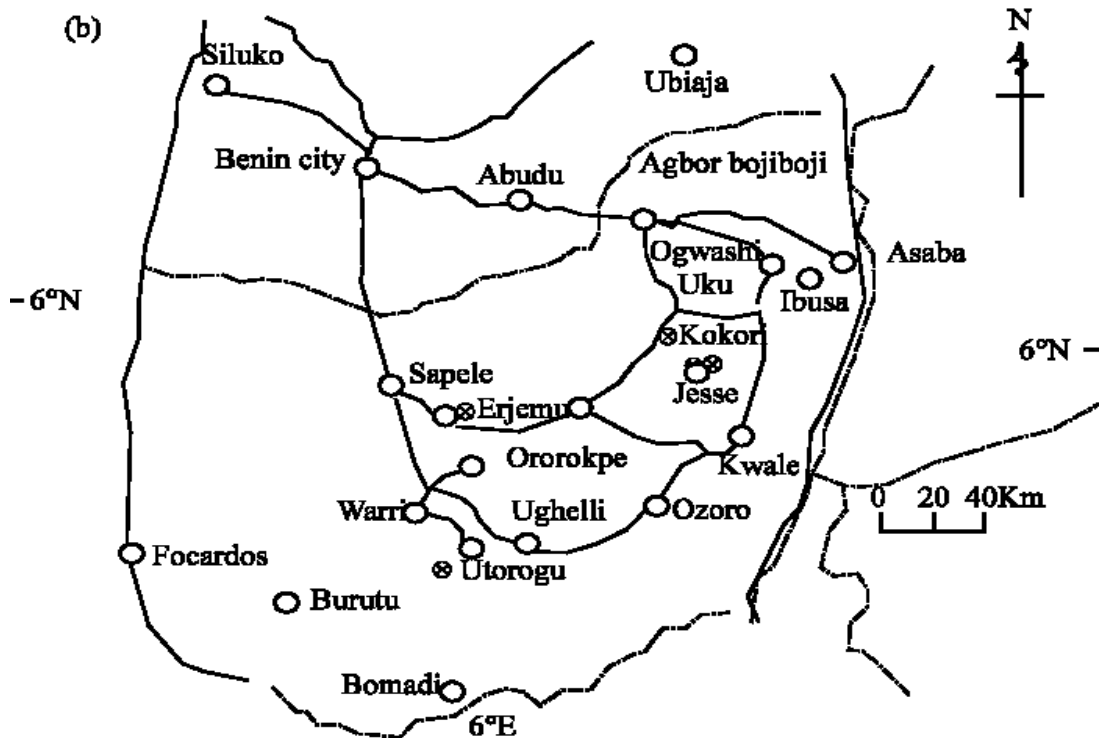


Figure 7: Niger Delta Region, Nigeria

Nigeria has a substantial reserve of paraffinic crude oils (Ajiienka and Ikoku, 1997), known for their good quality (low sulfur, high API gravity), and containing moderate to high contents of paraffinic waxes. The data correlated for light, medium and heavy crude oil samples from different sites in Nigeria show densities ranging from 0.813-0.849 g/ml, 0.866- 0.886 g/ml, and 0.925-.935 g/ml at 15°C respectively. Characteristically, waxy crude oil have undesirably high pour points and are difficult to handle where the flowing and ambient temperatures are about or less than the pour-point. They exhibit non-Newtonian flow behavior at temperatures below the cloud point due to wax crystallization. Consequently, the pipeline transportation of petroleum crude oil from the production wells to the refineries is threatened. In fact, pipelines have been known to wax up beyond recovery in Nigeria. Production tubing has also been known to wax up, necessitating frequent wax cutting, using scrapers conveyed by wire-line, which is an expensive practice. Billions of dollars have been lost to its prevention and remediation.

The main components of the heavy fraction, which participate in the solid phase formation, include asphaltenes, diamondoids, petroleum resins and wax. Petroleum wax consists mainly of saturated paraffin hydrocarbons with the number of carbon atoms in the range of 18–36. Wax may also contain small amounts of naphthenic hydrocarbons with their number of carbon atoms in the range of 30–60. Wax usually exists in intermediate crudes, heavy oils, tar sands and oil shale.

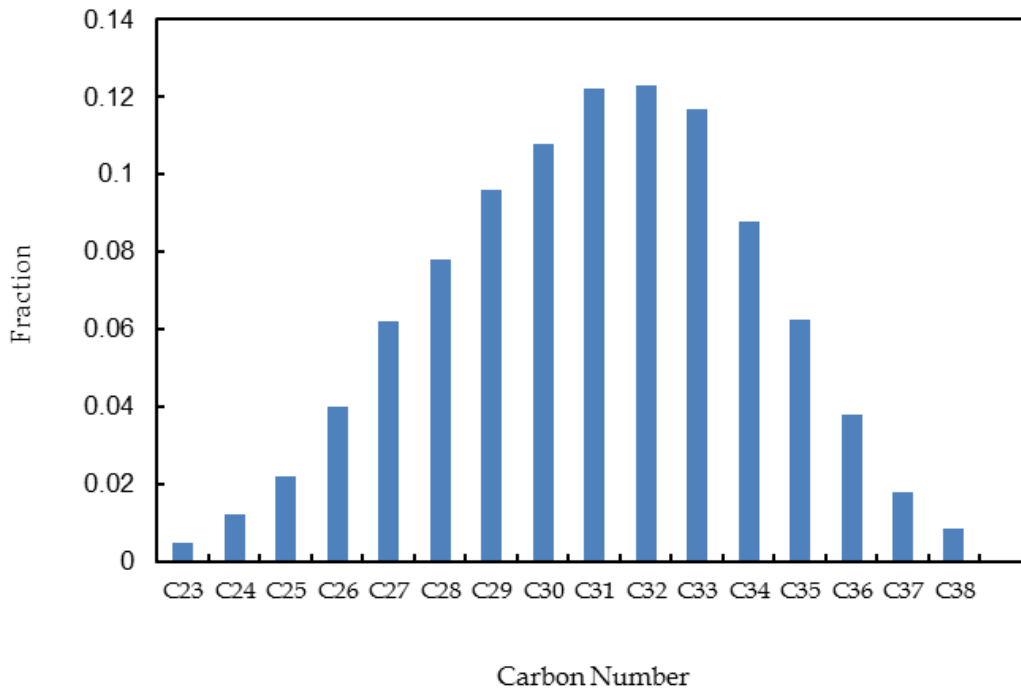


Figure 8: Carbon Number Distribution in Wax

To reduce the effect of deposition of wax in tubing & pipelines, SHELL is using permanent magnets in its equipment. These permanent magnets have high strengths and prevent the deposition of waxes in the down-hole equipment and pipelines. But these permanent magnets are very costly and make the down-hole system bulkier. Moreover, due to heat from the formation, those permanent magnets start losing their magnetic property over a period of time.

1.6. Effect of Magnetic Field on Less Paraffinic crude - Case Study of American Crude

This method was first implemented by Rongjia Tao in 2006. Rongjia Tao and his colleague Xiao Jun Xu took paraffin based crude from Sunoco Refinery and conducted experiments in Brookfield Viscometer whose spindle rotates with the speed of 10 RPM. The pour point of the sample was 17°C. The viscosity of the sample has been increased to 40.97 CP by reducing the temperature below its pour point i.e. 10°C. When the magnetic field of 1.33 Tesla is applied to it for 50 seconds at 10°C, the crude viscosity is reduced to 33.21 CP.

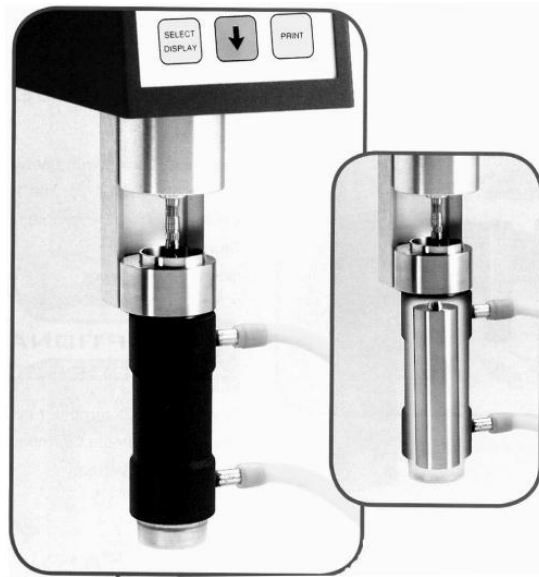


Figure 9: Brookfield Viscometer, UL adapter with a precision cylindrical spindle rotating inside

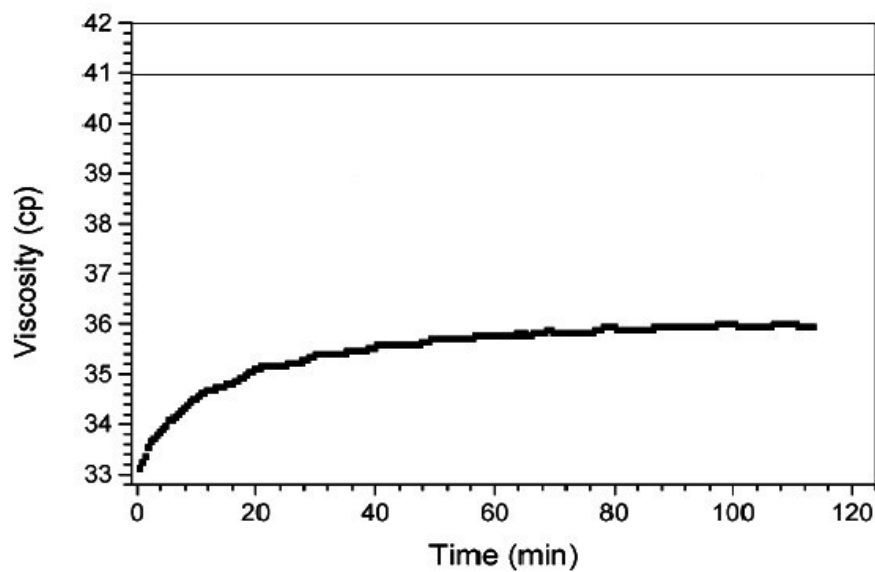


Figure 10: Viscosity – time curve of paraffin based crude oil sample at 10° C and 10 RPM was down to 33.1 CP from 40.97 CP after applying the magnetic field of 1.33 Tesla for 50 seconds (Source: Energy & Fuels 2006, 20)

They had observed that the original viscosity was retrieved in 8 hours after the removal of the magnetic field. Moreover, they had also found that if the same amount magnetic field was applied for 120 minutes it would substantially increase the viscosity of crude but in lower magnitude than the original value.

Working Mechanism

When the paraffinic crude particles come under the influence of strong magnetic field, the wax clusters are broken into shorter particles and align themselves in the direction of the field. Due to short particle size, less resistance offered by the adjacent layers of crude is reduced and less shear force is required which in turn lowers the viscosity of crude.

Limitation of his model

1. Rongjia Tao and his team performed the experiment in Brookfield Viscometer which was a vertical container of few centimeters in length and a few millimeters in diameter. But in practical application, the pipelines are spread over several hundred kilometers and are horizontally or inclined due to topography. So, the results obtained cannot be used to conclude that this approach would be applicable on transporting paraffin crude as no pilot experiment has been performed in pipelines even in the laboratory scale, with its length ranging from single digit feet to double digit feet and diameter of a few inches.
2. The sample used in that experiment was taken from Sunoco Refinery, Philadelphia, and it was light paraffinic oil (3-4 % Paraffin Content) with very low viscosity (40.97 cP at 10° C). His team didn't perform the experiment on more viscous paraffinic crude.
3. Moreover, in order to perform the experiment on elevated viscosity, he reduced the temperature 7° C below pour point of crude. The pour point of that crude was 17° C. Also, during the experiment, they have restricted the flow of crude. As we know that most of the world's crude are transported in liquid form without any restriction to flow. Therefore, before implementing on the pipeline scale, the experiment should be conducted again on ambient temperature.
4. Initial viscosity value and temperature was not mentioned. This shows that there is a need to re-conduct the experiment with paraffinic crude which possesses high viscosity at ambient temperature.
5. Last but not the least, the experimental setup for generating the magnetic field was not mentioned. This results in the confusion whether he choose a permanent magnet or an electromagnet for generating the magnetic field.

1.7. Viscosity Reduction using an Electromagnet – New Concept

Instead of wrapping permanent magnets over a pipeline, if an Electromagnet is wrapped then huge cost can be saved and it will reduce the bulkiness of the pipeline. As we know that the current flowing through a coiled wire produces a magnetic field. When a solenoid type wire is wrapped over the pipeline, it will produce the working mechanism similar to that of the permanent magnets. The additional advantage offered by an electromagnet is that due to change in the polarity of current it will simultaneously breaks the film of paraffin particles which lowers the surface tension of crude. Due to this the relaxation modulus crude starts decreasing exponentially. This results in the decrease in pressure drop caused by the flow of viscous crude in the pipelines.

1.7.1. Advantage over Permanent Magnets

Some of the advantages have been discussed of using electromagnets as a source of producing magnetic field.

1. Easy to construct and more economical as it requires copper wire only. Permanent magnets on the other hand are very costly (approx. 150,000 INR per meter).
2. The electromagnets won't make the pipelines bulky.
3. By increasing or decreasing the number of turns and the magnitude of current, the magnetic field of electromagnet can be varied. This gives it flexibility in producing magnetic field as per the requirement. On the other hand, the field strength of permanent magnets cannot be varied.
4. The electromagnets are more powerful magnet than permanent magnets.
5. The permanent magnet loses their magnetic property when subjected to elevated temperatures or pressures. This problem is to be observed in the down-hole equipment (from Nigerian case study). While there is no case of losing field strength as they are the function of current and coil numbers. Hence they can be installed in down-hole equipment also.
6. Last but not the least, the permanent magnets as susceptible to the sudden vibrations and shocks as results in the decline in the field strength of particles. Therefore, it is to be taken in account that flow of crude is maintained at specific rate. Whereas, this problem is rectified in case of an electromagnets.

1.8. Modified Scheme for Pilot Experiment using an Electromagnet

It is proposed that a new experimental set up which would replicate a field pipeline for pilot experiment with a paraffinic crude oil. This experiment would comprise of two sections: static and run time section. The static experiment aims to validate the outcomes of Tao's result. If the viscosity is found to be decreased due to high magnetic field in static test, then the experiment is taken to the dynamic stage where the validity of magnetic field effect has to be checked in flowing condition. The basic apparatus in static test includes a Hall Effect magnetic sensor probe, a gauss meter, an electromagnet and a Rheometer. A temperature bath is installed with the Rheometer in order to maintain a constant temperature throughout the experiment. In dynamic run, apart from these above mentioned instruments, a piping system, flow control valve and an insulating material is required which would impart free flow of crude through the oil source. The specifications and details of material used during the experiment have been discussed in the upcoming chapters along with their operating procedures. The results from these two experiments can be further extended to the industrial point of application for transporting paraffinic crude in pipelines through electromagnets.

Chapter 2: Static Experimental Run

2.1.Design of Experimental Setup for Static Run

The purpose of static run was to validate the results of Rongjia Tao's experiment with our experiment. Therefore, two sets of designs were proposed to conduct static experiment. In the first layout, crude is subjected to a container which would itself behave as an electromagnet. However, in the second layout, a crude carrying container is kept in between the two poles of magnetic field. These two designs have been discussed below:

2.1.1. Theoretical Design of Apparatus 1

The theoretical design of experimental setup of was consist of a container wrapped with a copper coil, a Hall Effect magnetic field sensor probe, a gauss meter and a Rheostat. A hollow mild steel container with 2 inch OD and 30 cm (approx. 1 ft.) in length with G.I. (Galvanized Iron) coating was taken to conduct the experiment. The bottom of container was closed in order to store the crude in it. The purpose of taking mild steel as a material of construction is that most of the crude oil pipelines are made up of mild steel and conducting experiment on it would give us the best result on oil flow behavior during dynamic run.

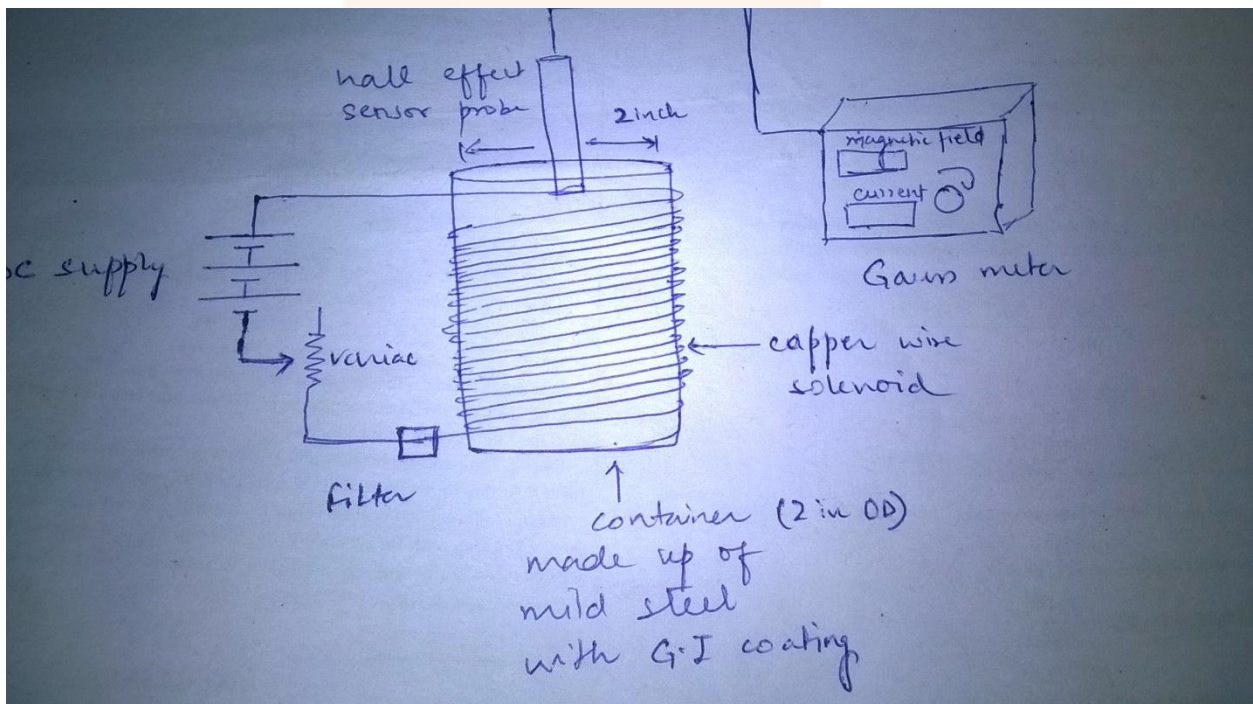


Figure 11: Theoretical Design of Apparatus 1

A copper wire of 28 gauge diameter is to be wrapped (1500 turns) in the bobbin made up of same material (i.e. mild steel). A DC supply source along with the Rheostat is to be connected with the two ends of copper wire in order to provide current for generation of magnetic field inside the container.



Figure 12: Structure of Apparatus 1

Once the current was started flowing through the copper coil, it generated magnetic field lines inside the container which were regular and convergent inside the container whereas irregular and divergent outside the container. At the center of the container, the magnetic field had its maximum value.

2.1.2. Failure of Apparatus 1

The Apparatus 1 was producing magnetic field of magnitude 40 Gauss (4 mT) at the corner and 80 Gauss (8 mT) at the center when connected to DC supply of 220 V and 3.67 Amperes current (max permissible value) flowing through it. But fairly high magnetic field ranging from 5000 Gauss (0.5 Tesla) to 1.5 Tesla was required to break the clusters of paraffinic particles and align them in straight line.

The reason behind producing low magnetic field was due to the presence of air as a medium inside the container. The magnetic permeability of air is $4\pi \times 10^{-7}$ H/m which is closed to vacuum. The gaseous particles present in air are mostly diamagnetic (like N_2) or paramagnetic (like O_2) in nature. The magnetic field has no effect on diamagnetic substances whereas it aligns the paramagnetic particles for very short period of time.

Since the diameter of the container was 2 inch, therefore huge air medium restricts the formation of stronger magnetic field. Therefore, in despite of producing magnetic field, the Apparatus 1 was not suitable for conducting the static test.

2.1.3. Technical Outcomes from the Failures and Theoretical Design of Apparatus 2

In order to overcome the flaws from the Apparatus 1, a new design of experimental apparatus was presented. The mathematical equation for the magnetic field for a solenoid is given as:

$$B = \mu n I = \frac{\mu N I}{L}$$

Where, μ = Magnetic permeability of the substance

n = Number of turns per unit length

I = Current flowing through the wire

N = Total number of turns

L = Length

Therefore, keeping these parameters in mind, following modifications were made in the design.

1. Instead of mild steel, Wrought Iron (98.8 % Pure Iron) was to be taken as a material of construction. The relative permeability of mild steel is 100 times to that of absolute vacuum whereas Wrought iron has the relative permeability of the 5000 times to that of vacuum. Thus the magnetic field formed from the pure Iron is 50 times stronger than that of mild steel for the same no of turns and current.
2. The air gap inside the container was reduced by reducing the diameter of container by installing wrought iron core in it. Thus the resistance offered to magnetic field lines can be reduced.
3. The magnetic field could be increased by increasing the current. In order to increase the current, the gauge of wire is reduced (i.e. diameter of wire is increased). Due to more area of the wire, more current was consumed and stronger electromagnet could be made (as per the following equation).

$$R = \rho \frac{L}{A} = \frac{V}{I}$$

Where, ρ = resistivity of wire

L = Length of wire

A = Cross sectional area of wire (more area, less resistance and more current)

V = Voltage

4. Moreover, due to high current, heating of coil could happen (as per Joule's Law of Heating). Therefore, the number of turns had to be increased (up to 2500 turns) in order to consume whole current within the system.

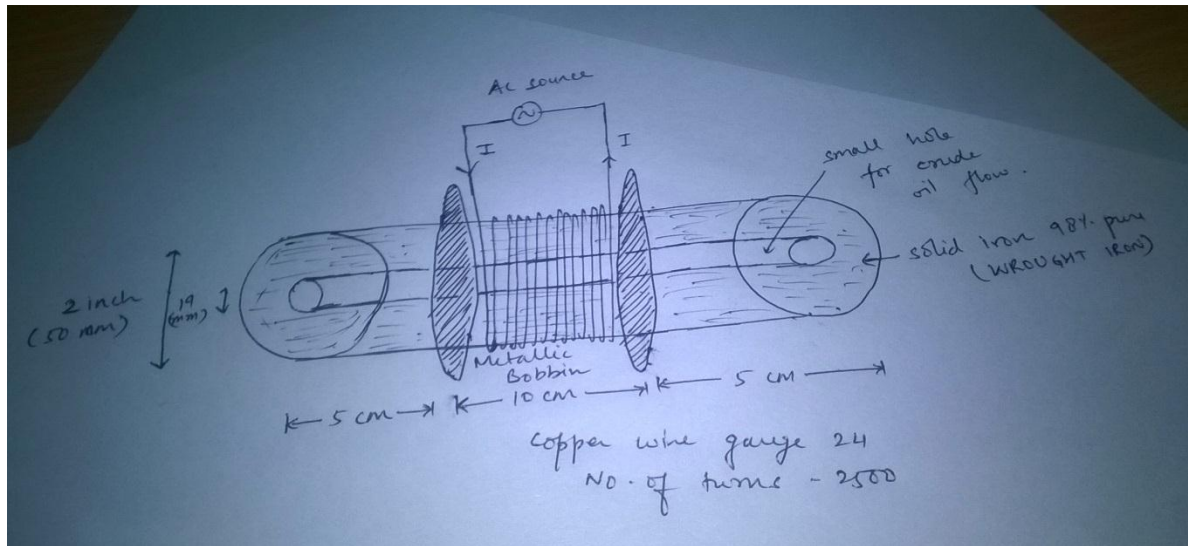


Figure 13: Theoretical Design of Apparatus 2

In this design, direct AC supply was given. For solenoid type electromagnet, DC current shouldn't be provided because it will short the circuit. It can be explained by the following equation:

$$X_L = \omega L = 2\pi fL = \frac{V}{I}$$

Where, ω = Angular frequency

L = Inductance of wire

f = frequency

We know that the frequency of DC current is zero; therefore the value of impedance offered by the solenoid or the copper coil is also zero. This makes the value of current as infinity which would cause short circuiting. In Apparatus 1, DC source is supplied because that was integrated with filter in it to prevent the shorting of circuit.



Figure 14: Structure of Apparatus 2

For constructing Apparatus 2, a solid wrought iron rod with 2 inch (50 mm) OD and 8 inch (21 cm) in length is taken. In order to reduce the air gap, a hole of 19 mm is made from the drill in the direction of rod's axis. Then, with the same material, two circular discs have been welded with the clearances of 5 cm from both the ends of the rod, so that we can have a metallic bobbin. Then, a thin PVC sheet was wrapped over the entire bobbin to prevent the short circuiting of the rod with the wire. Moreover, a white insulated paint has been sprayed in the metallic rod to prevent the flow of current in entire rod. Afterwards, the copper coil of 24 gauges dia. is wrapped with 2500 turns and finally varnished with the paint.

2.1.4. Limitation of Hall Effect Magnetic Field Sensor and Uncertainty in Apparatus 2

The Apparatus 2 was developing good magnetic field due to Wrought Iron Core and Air Gap Reduction. Due to increase in the diameter of the coil, the current consumption was increased. For 220 V and 4.23 Ampère current, it was producing Magnetic field of 2500 Gauss (0.25 Tesla) at the corner.

Due to the limitation of the Hall Effect Sensor, we couldn't determine the magnetic field inside the core. The sensor probe only measures the magnetic field at its perpendicular orientation. If it is inserted in the direction parallel to the magnetic field, then it would not sense any magnetic field. When the air gap was eliminated by the Wrought Iron Core, then it became impossible to insert the sensor probe at the center in the radial direction. This can be explained by the following diagram.

This results in the uncertainty whether the magnetic field produced at the center has been achieved or not. Therefore, despite in the success of producing high magnetic high (of order 0.25 Tesla at the tip) we have to reject this apparatus.

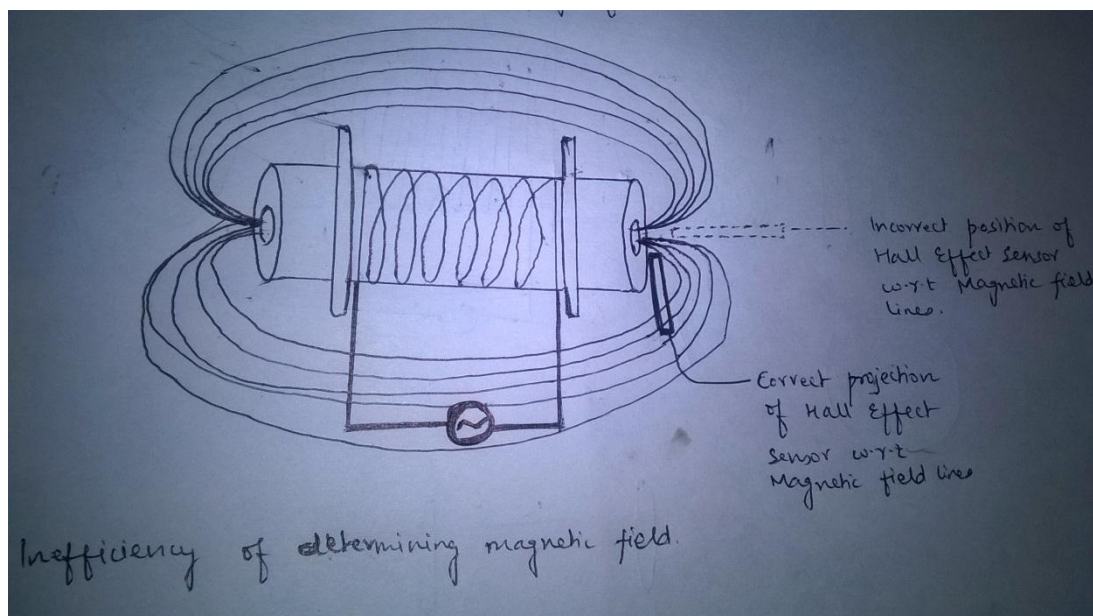


Figure 15: Limitation of Hall Effect Sensor in Sensing Magnetic Field at the Center

2.1.5. Apparatus 3 for Static Test

The apparatus 3 consists of Hall Effect equipment for generation of magnetic field, a sensor probe, a digital gauss meter, a sensor probe and a DC power source. This setup is different from the previous setup in two ways:

1. Unlike previous two setups, this one consists of two poles which are made by winding copper wires on soft iron core.
2. Secondly, instead of using wrapping the mild steel pipeline with coil, we have placed a glass test tube between the two poles of magnet.



Figure 16: Hall Effect Equipment and Accessories (684 x10 Gauss reading at 2.86 Ampere Current with 1.25 Inch Air Gap Between the two poles of Electromagnet)

Performing experiment on this setup gave desired magnitude of field required to execute the procedure. The upper limit of magnetic field is 1.25 Tesla (for least air gap).

2.2.Procedure for Static Test

The procedure for the static test has been discussed below:

1. As the crude which we have used has some water present in it, therefore there is need to remove water. Thus, the entire crude sample was heated for 6 hours at 80° C in Air Driven Oven and then allowed to cool for next 2 hours at ambient temperature. During this period the crude was solidified at the top (as pour point of crude was 35° C) and water is removed from the bottom.

2. As the objective of the experiment is to treat the crude above the pour point, therefore, then crude is heated up to 46° C (treating temperature). The temperature of water bath is maintained few degrees above the treating temperature i.e. at 50° C.
3. Then the crude is treated for 1 minute at different magnetic fields (6500 Gauss, etc.) at 46° C i.e. at treating temperature.
4. Since there is some temperature loss during the magnetic conditioning, therefore the crude is again reheated to 46° C before keeping it into the Rheometer.
5. Finally the crude is placed inside Rheometer to understand the Rheology of crude after magnetic treatment.

The next chapter deals with the experimental outcomes of the static test.



Chapter 3: Observations & Outcomes from Static Experiment

3.1. Viscometer Calibration

Before performing experiment, the first step was to calibrate the viscometer in order to reduce the experimental error. Therefore, the Laboratory data which we have taken from ONGC was rechecked by doing interpolation and then comparing it with the viscometer reading at that temperature.

3.1.1. Interpolation of Laboratory's Data at 46° C Temperature

As per the data sheet provided by the company, the viscosity of crude is varied from 10° C temperature scale at constant 34 s⁻¹ shear rate. The pour point of the crude was 33° C and wax content is about 24 – 27 % by weight. Since the treating temperature of crude was 46° C, therefore upper limit of temperature was taken as 50° C and lower limit as 40° C for doing the interpolation at 46° C.

No. BICP/CHEM/OIL/43/2013

Description of sample

Type of sample	: Oil-emulsion
Source	: Mewad # 37
Collected on	: 31.08.13
Received in lab. on	: 02.09.13
Tested by	: Area Manager, Sobhasan Area

Analysis data

Sr. No.	Parameters of emulsion	
1	Free water content (%v/v)	Nil
2	Water content (%v/v)	60.0
3	Total water content (%v/v)	60.0
4	Viscosity data	
	Temperature (°C)	Viscosity (cP) @ Shear Rate 34.0 s ⁻¹
	30	Out of scale
	40	247
	50	143
	60	80
	70	57
	Parameters of dehydrated oil	
	Water content (%v/v)	0.8
	Density at 15°C (g/cc)	0.8919
	API gravity (deg)	27.1
	Pour point (°C)	33
	Viscosity data	
	Temperature (°C)	Viscosity (cP) @ Shear Rate 34.0 s ⁻¹
	30	242
	40	90
	50	56
	60	33
	70	21

ruah
5.9.13
ruah

B.

Figure 17: Viscosity Details of Crude at Different Temperatures

It can be seen in the above table that the viscosity of dehydrated oil was 90 cP at 40°C and 56 cP at 50° C temperature. Therefore, the viscosity of crude at 46° C can be interpolated as:

$$\mu_{at\ 46} = \left[\mu_{at\ 50} + \left(\frac{T_{at\ 46} - T_{at\ 40}}{T_{at\ 50} - T_{at\ 40}} \right) (\mu_{at\ 40} - \mu_{at\ 50}) \right]$$

Putting the value in the formula we have

$$\mu_{at\ 46} = \left[56 + \left(\frac{46 - 50}{40 - 50} \right) (90 - 56) \right]$$

$$\mu_{at\ 46} = 69.6\ cP$$

Thus the interpolated viscosity of crude oil at 46° C temperature was 69.6 cP

3.2. Readings at 7500 Gauss Magnetic Field

Three sets of reading has been taken by subjecting crude under the magnetic field of 7500 Gauss magnetic field.

3.2.1. Initial Reading

Table 1: Reading 1 at 7500 Gauss

Meas. Pts.	Time	Viscosity	Temperature	Shear Rate	Shear Stress	Torque
	[s]	[cP]	[°C]	[1/s]	[Pa]	[mNm]
1	600	20.4	46.2	34	0.354	0.0596
2	1,200	20.4	46.3	34	0.355	0.0596
3	1,800	20.8	46.3	34	0.367	0.0617
4	2,400	20.9	46.4	34	0.371	0.0624
5	3,000	21	46.3	34	0.373	0.0628
6	3,600	20.5	46.3	34	0.356	0.0599
7	4,200	20.4	46.4	34	0.355	0.0597
8	4,800	20.4	46.3	34	0.353	0.0593
9	5,400	20.7	46.3	34	0.365	0.0614
10	6,000	20.7	46.3	34	0.365	0.0614
11	6,600	20.1	46.4	34	0.344	0.0579
12	7,200	20.3	46.4	34	0.352	0.0591
13	7,800	20.2	46.3	34	0.346	0.0581
14	8,400	20.1	46.4	34	0.345	0.058
15	9,000	21	46.4	34	0.373	0.0627

3.2.2. Second Reading

Table 2: Reading 2 at 7500 Gauss

Meas. Pts.	Time	Viscosity	Temperature	Shear Rate	Shear Stress	Torque
	[s]	[cP]	[°C]	[1/s]	[Pa]	[mNm]
1	600	23.9	46.3	34	0.472	0.0793
2	1,200	23.7	46.3	34	0.466	0.0784
3	1,800	23.7	46.3	34	0.467	0.0786
4	2,400	24.1	46.4	34	0.478	0.0803
5	3,000	24.2	46.4	34	0.483	0.0811
6	3,600	24.4	46.5	34	0.489	0.0822
7	4,200	24.5	46.4	34	0.493	0.0828
8	4,800	24.6	46.5	34	0.495	0.0832
9	5,400	25.1	46.4	34	0.514	0.0864
10	6,000	25	46.5	34	0.509	0.0856
11	6,600	25	46.6	34	0.511	0.0858
12	7,200	24.1	46.4	34	0.478	0.0804
13	7,800	24.1	46.5	34	0.48	0.0807
14	8,400	24.3	46.5	34	0.48	0.0807
15	9,000	24.4	46.5	34	0.48	0.0807

3.2.3. Third Reading

Table 3: Reading 3 at 7500 Gauss

Meas. Pts.	Time	Viscosity	Temperature	Shear Rate	Shear Stress	Torque
	[s]	[cP]	[°C]	[1/s]	[Pa]	[mNm]
1	600	21.4	46.4	34	0.387	0.065
2	1,200	21.8	46.3	34	0.403	0.0677
3	1,800	21.8	46.4	34	0.401	0.0673
4	2,400	21.8	46.4	34	0.403	0.0677
5	3,000	21.9	46.3	34	0.404	0.0679
6	3,600	22	46.4	34	0.408	0.0687
7	4,200	22	46.3	34	0.408	0.0685
8	4,800	22.3	46.3	34	0.419	0.0705
9	5,400	22.3	46.3	34	0.419	0.0705
10	6,000	23.1	46.4	34	0.445	0.0749
11	6,600	22.8	46.4	34	0.434	0.0729
12	7,200	22.1	46.4	34	0.411	0.0691
13	7,800	22.1	46.3	34	0.41	0.0689
14	8,400	21.5	46.3	34	0.392	0.0659
15	9,000	21.3	46.4	34	0.385	0.0647

3.2.4. Conclusion from Magnetic Treating at 7500 Gauss

Table 4: Compiled Reading at 7500 Gauss

Meas. Pts.	Time	Untreated Crude's Viscosity	Viscosity 1	Viscosity 2	Viscosity 3
	[s]	[cP]	[cP]	[cP]	[cP]
1	600	60.6	20.4	23.9	21.4
2	1,200	61	20.4	23.7	21.8
3	1,800	62	20.8	23.7	21.8
4	2,400	62.1	20.9	24.1	21.8
5	3,000	61.5	21	24.2	21.9
6	3,600	61.5	20.5	24.4	22
7	4,200	61.9	20.4	24.5	22
8	4,800	61.3	20.4	24.6	22.3
9	5,400	60.1	20.7	25.1	22.3
10	6,000	59.2	20.7	25	23.1
11	6,600	61.5	20.1	25	22.8
12	7,200	60.9	20.3	24.1	22.1
13	7,800	61.1	20.2	24.1	22.1
14	8,400	61.8	20.1	24.3	21.5
15	9,000	62.3	21	24.4	21.3

THE NATION BUILDERS UNIVERSITY

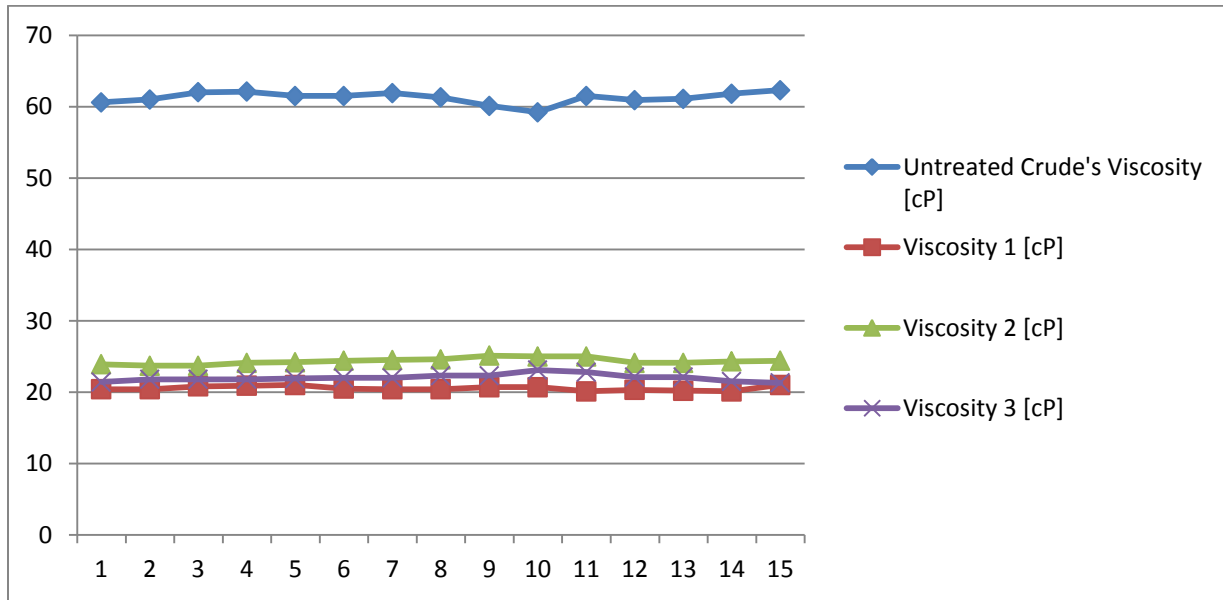


Figure 18: Comparison of Viscosity before treating and after treating at 7500 Gauss Magnetic Field

From above data and graph, rough estimations can be made regarding the viscosity reduction of crude after the magnetic treatment.

% Viscosity Decline

$$= \left(\frac{\text{Viscosity of Untreated Sample} - \text{Viscosity of Treated Sample}}{\text{Viscosity of Untreated Sample}} \right) 100$$

$$= \left(\frac{61.2 - 21.2}{61.2} \right) \times 100$$

$$= 65.34 \% \text{ decline in the viscosity}$$

3.3. Readings at 6800 Gauss

Three sets of reading has been taken by subjecting crude under the magnetic field of 6800 Gauss magnetic field.

3.3.1. Initial Reading

Table 5: Reading 1 at 6800 Gauss

Meas. Pts.	Time	Viscosity	Temperature	Shear Stress	Torque	Relaxation Modulus
	[s]	[cP]	[°C]	[Pa]	[mNm]	[Pa]
1	600	27.7	46.4	0.941	0.158	0.0000612
2	1,200	25.8	46.4	0.878	0.147	0.0000245
3	1,800	25.7	46.5	0.874	0.147	0.0000156
4	2,400	24.8	46.5	0.844	0.142	0.000011
5	3,000	25	46.4	0.85	0.143	0.00000874
6	3,600	24.8	46.5	0.844	0.142	0.00000716
7	4,200	24.3	46.5	0.826	0.139	0.00000597
8	4,800	23.9	46.4	0.814	0.137	0.00000512
9	5,400	24.3	46.5	0.826	0.139	0.0000046
10	6,000	23.9	46.5	0.811	0.136	0.00000406
11	6,600	23.6	46.5	0.802	0.135	0.00000364
12	7,200	24.7	46.5	0.84	0.141	0.00000348
13	7,800	24	46.5	0.816	0.137	0.00000312
14	8,400	23.6	46.5	0.801	0.135	0.00000284
15	9,000	23.3	46.5	0.792	0.133	0.00000262

3.3.2. Second Reading

Table 6: Reading 2 at 6800 Gauss

Meas. Pts.	Time	Viscosity	Temperature	Shear Stress	Torque	Relaxation Modulus
	[s]	[cP]	[°C]	[Pa]	[mNm]	[Pa]
1	600	25.2	46.6	0.857	0.144	0.0000559
2	1,200	23.5	46.5	0.8	0.134	0.0000224
3	1,800	22.2	46.6	0.756	0.127	0.0000135
4	2,400	21.3	46.6	0.725	0.122	0.00000947
5	3,000	21.1	46.4	0.717	0.12	0.00000739
6	3,600	21.4	46.5	0.726	0.122	0.00000619
7	4,200	20.9	46.6	0.712	0.12	0.00000517
8	4,800	21.3	46.6	0.724	0.122	0.00000458
9	5,400	21.6	46.4	0.736	0.124	0.00000412
10	6,000	20.7	46.4	0.703	0.118	0.00000353
11	6,600	21.7	46.4	0.738	0.124	0.00000337
12	7,200	22.1	46.4	0.752	0.126	0.00000314
13	7,800	21.4	46.4	0.727	0.122	0.00000279
14	8,400	21.1	46.4	0.719	0.121	0.00000256
15	9,000	20.9	46.4	0.711	0.119	0.00000236

3.3.3. Third Reading

Table 7: Reading 3 at 6800 Gauss

Meas. Pts.	Time	Viscosity	Temperature	Shear Stress	Torque	Relaxation Modulus
	[s]	[cP]	[°C]	[Pa]	[mNm]	[Pa]
1	600	30.5	46.4	0.804	0.135	0.0000523
2	1,200	26.1	46.5	0.715	0.12	0.00002
3	1,800	25.3	46.5	0.705	0.119	0.0000126
4	2,400	24.7	46.5	0.696	0.117	0.00000909
5	3,000	24.3	46.6	0.689	0.116	0.00000711
6	3,600	23.9	46.6	0.677	0.114	0.00000577
7	4,200	23.7	46.6	0.681	0.115	0.00000495
8	4,800	23.4	46.5	0.683	0.115	0.00000432
9	5,400	23.4	46.5	0.675	0.113	0.00000378
10	6,000	23.6	46.4	0.662	0.111	0.00000333
11	6,600	23.6	46.4	0.647	0.109	0.00000295
12	7,200	23.7	46.4	0.642	0.108	0.00000268
13	7,800	22.8	46.4	0.627	0.105	0.00000241
14	8,400	23	46.4	0.622	0.104	0.00000222
15	9,000	22.8	46.4	0.63	0.106	0.00000209

3.3.4. Conclusion from Magnetic Treating at 6800 Gauss

Table 8: Compiled Reading at 6800 Gauss

Meas. Pts.	Time	Untreated Crude's Viscosity	Viscosity 1	Viscosity 2	Viscosity 3
	[s]	[cP]	[cP]	[cP]	[cP]
1	600	60.6	27.7	25.2	30.5
2	1,200	61	25.8	23.5	26.1
3	1,800	62	25.7	22.2	25.3
4	2,400	62.1	24.8	21.3	24.7
5	3,000	61.5	25	21.1	24.3
6	3,600	61.5	24.8	21.4	23.9
7	4,200	61.9	24.3	20.9	23.7
8	4,800	61.3	23.9	21.3	23.4
9	5,400	60.1	24.3	21.6	23.4
10	6,000	59.2	23.9	20.7	23.6
11	6,600	61.5	23.6	21.7	23.6
12	7,200	60.9	24.7	22.1	23.7
13	7,800	61.1	24	21.4	22.8
14	8,400	61.8	23.6	21.1	23
15	9,000	62.3	23.3	20.9	22.8

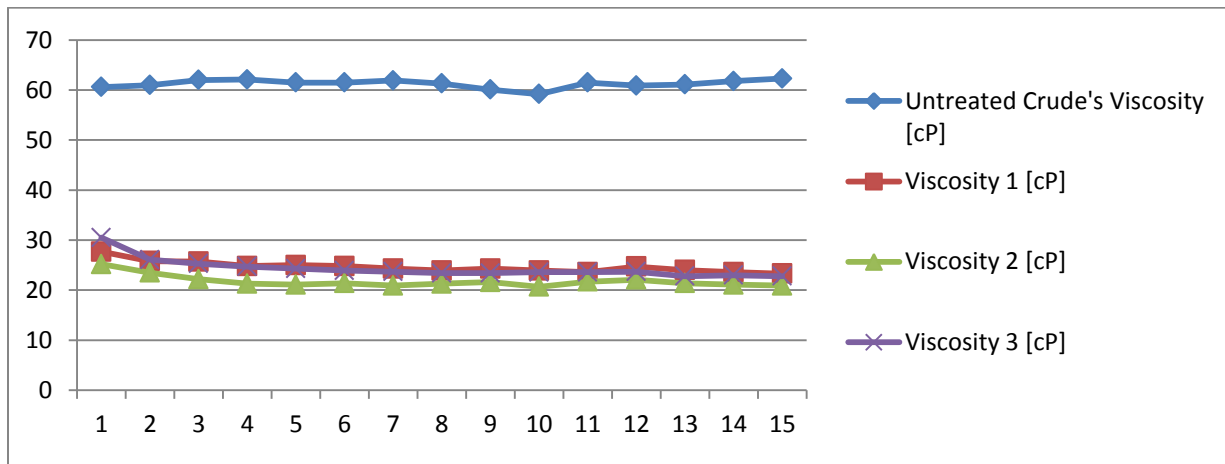


Figure 19: Comparison of Viscosity before treating and after treating at 6800 Gauss Magnetic Field

From above data and graph, rough estimations can be made regarding the viscosity reduction of crude after the magnetic treatment.

$$\% \text{ Viscosity Decline} = \left(\frac{61.2 - 25.2}{61.2} \right) \times 100$$

$$= 58.82 \% \text{ decline in the viscosity}$$

This % decline is less than that of previous magnetic field (i.e. at 7500 Gauss). This could happen due to less strength field in the field which leads to fewer breakdowns of paraffinic particles. Also from above 3 data series we can find the relaxation modulus (or bulk modulus) of crude is decreasing exponentially.

Table 9: Compiled Relaxation Modulus Data at 6800 Gauss Magnetic Field

Meas. Pts.	Time [s]	Relaxation Modulus 1 [Pa]	Relaxation Modulus 2 [Pa]	Relaxation Modulus 3 [Pa]
1	600	0.0000612	0.0000559	0.0000523
2	1,200	0.0000245	0.0000224	0.00002
3	1,800	0.0000156	0.0000135	0.0000126
4	2,400	0.000011	0.00000947	0.00000909
5	3,000	0.00000874	0.00000739	0.00000711
6	3,600	0.00000716	0.00000619	0.00000577
7	4,200	0.00000597	0.00000517	0.00000495
8	4,800	0.00000512	0.00000458	0.00000432
9	5,400	0.0000046	0.00000412	0.00000378
10	6,000	0.00000406	0.00000353	0.00000333
11	6,600	0.00000364	0.00000337	0.00000295
12	7,200	0.00000348	0.00000314	0.00000268
13	7,800	0.00000312	0.00000279	0.00000241
14	8,400	0.00000284	0.00000256	0.00000222
15	9,000	0.00000262	0.00000236	0.00000209

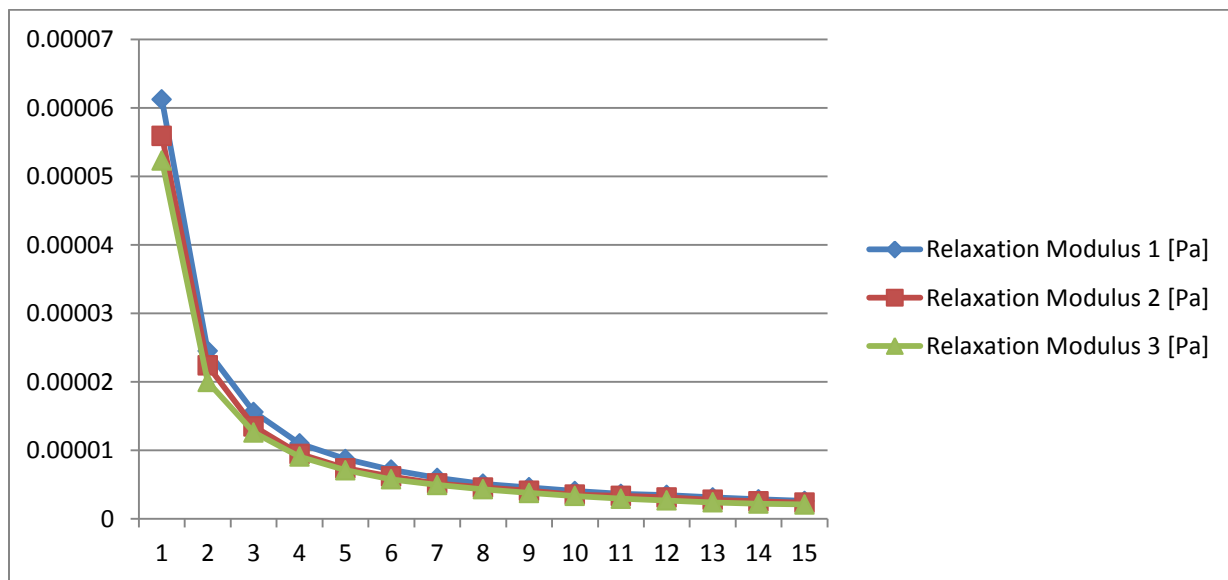


Figure 20: Behavior of Relaxation Modulus of Crude after treating in Magnetic Field of 6800 Gauss

This graph shows that the paraffinic crude which we are conducting an experiment is viscoelastic in nature. That means on providing constant shear rate and shear stress, the bulk modulus will decline exponentially with time. This property of crude would provide ease in the transportation by lowering the outlet pressure.

It can be explained by the following equations:

$$\text{Bulk Modulus} = \frac{\text{Pressure}}{\text{Volumetric Strain}} = \frac{-1}{\text{Compressibility}}$$

Or mathematically

$$B = \left[\frac{P}{\left(\frac{\partial V}{\partial V} \right)} \right] = \frac{-1}{K}$$

Now as the value of B decreases, the corresponding P exerted on crude will also decrease. Therefore the outlet pressure of crude will decrease. Due to decrease in pipeline's outlet pressure, the pressure drop inside the pipeline would increase. This would enhance the flow ability of crude after the magnetic treatment.

Apart from these two results, it has been found that the deflection angle between crude and sensor probe is also increasing in a ramp manner after magnetic treating. This increment in the contact angle would solve the problem of wax deposition or sticking in the walls of pipeline.

Table 10: Compiled Deflection Angle Data at 6800 Gauss Magnetic Field

Meas. Pts.	Time [s]	Deflection Angle 1 [mrad]	Deflection Angle 2 [mrad]	Deflection Angle 3 [mrad]
1	600	1.24E+06	1.24E+06	1.25E+06
2	1,200	2.90E+06	2.90E+06	2.90E+06
3	1,800	4.55E+06	4.55E+06	4.56E+06
4	2,400	6.21E+06	6.21E+06	6.21E+06
5	3,000	7.86E+06	7.86E+06	7.87E+06
6	3,600	9.52E+06	9.52E+06	9.53E+06
7	4,200	1.12E+07	1.12E+07	1.12E+07
8	4,800	1.28E+07	1.28E+07	1.28E+07
9	5,400	1.45E+07	1.45E+07	1.45E+07
10	6,000	1.61E+07	1.61E+07	1.61E+07
11	6,600	1.78E+07	1.78E+07	1.78E+07
12	7,200	1.95E+07	1.95E+07	1.95E+07
13	7,800	2.11E+07	2.11E+07	2.11E+07
14	8,400	2.28E+07	2.28E+07	2.28E+07
15	9,000	2.44E+07	2.44E+07	2.44E+07

The possible reason behind the increase in the deflection angle with respect to sensor probe is decrease in surface tension. At microscopic level, due to breakdown of heavier paraffinic particles into smaller clusters, there is increase in randomness and decrease in surface tension. This increases the contact angle of crude which results in decline in the wettability by the crude and hence prevents the deposition of wax in pipeline.

It can also be explained by the mathematical expression for capillary (as container diameter was about 2 inches and probe's diameter is about 1.5 inches)

$$h = \frac{2 \sigma \cos \theta}{\rho g d}$$

Where σ is surface tension

θ is contact angle

ρ is density of liquid

h is height of column

g is acceleration due to gravity

d is diameter of container

As the value of σ decreases, there is increase in value of θ in terms of cosine. Thus the graph obtained from the above data is shown below

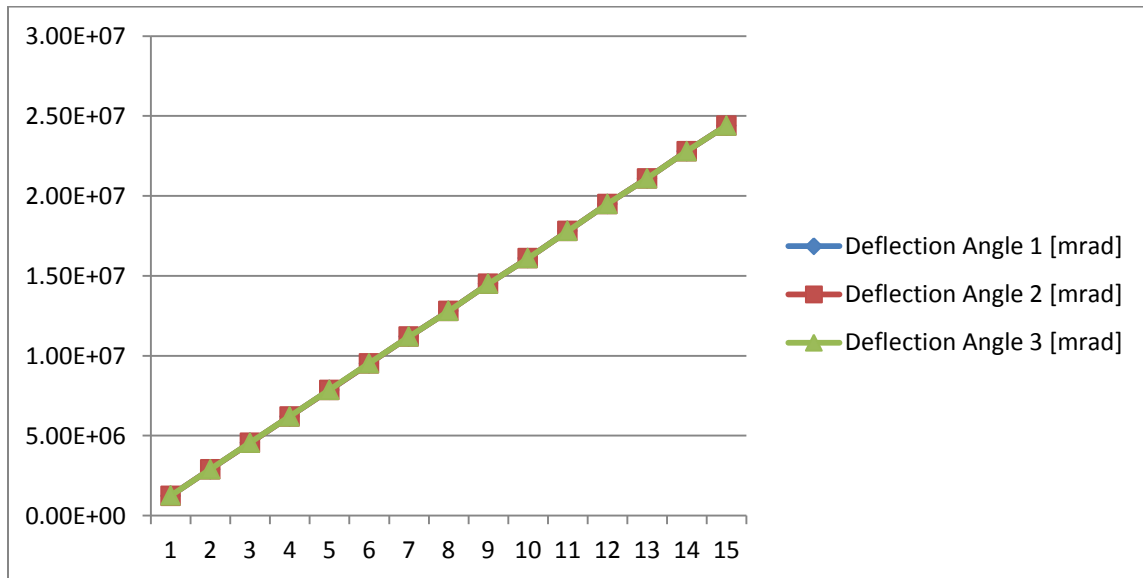


Figure 21: Behavior of Deflection Angle of Crude after treating in Magnetic Field of 6800 Gauss

3.4. Readings at 6500 Gauss

3.4.1. Initial Reading

Table 11: Reading 1 at 6500 Gauss Magnetic Field

Meas. Pts.	Time	Viscosity	Temperature	Shear Stress	Torque	Relaxation Modulus
	[s]	[cP]	[°C]	[Pa]	[mNm]	[Pa]
1	600	26.5	46.5	0.9	0.151	0.0000586
2	1,200	22	46.5	0.749	0.126	0.000021
3	1,800	21	46.6	0.716	0.12	0.0000127
4	2,400	20.7	46.6	0.702	0.118	0.00000918
5	3,000	20.4	46.6	0.695	0.117	0.00000717
6	3,600	20.4	46.7	0.694	0.117	0.00000591
7	4,200	20.4	46.7	0.694	0.117	0.00000504
8	4,800	20.7	46.7	0.703	0.118	0.00000445
9	5,400	20.6	46.8	0.701	0.118	0.00000392
10	6,000	20.4	46.8	0.693	0.116	0.00000348
11	6,600	20.1	46.8	0.682	0.115	0.00000311
12	7,200	20.3	46.7	0.691	0.116	0.00000288
13	7,800	20.3	46.7	0.689	0.116	0.00000265
14	8,400	18	46.6	0.613	0.103	0.00000219
15	9,000	18.2	46.6	0.619	0.104	0.00000206

3.4.2. Second Reading

Table 12: Reading 2 at 6500 Gauss

Meas. Pts.	Time	Viscosity	Temperature	Shear Stress	Torque	Relaxation Modulus
	[s]	[cP]	[°C]	[Pa]	[mNm]	[Pa]
1	600	33.6	46.2	1.14	0.192	0.0000745
2	1,200	27.5	46.3	0.936	0.157	0.0000262
3	1,800	25.2	46.4	0.857	0.144	0.0000153
4	2,400	25.3	46.4	0.862	0.145	0.0000113
5	3,000	25.1	46.5	0.852	0.143	0.00000879
6	3,600	24.6	46.5	0.835	0.14	0.00000712
7	4,200	24.2	46.5	0.824	0.139	0.00000598
8	4,800	24	46.6	0.815	0.137	0.00000516
9	5,400	23.7	46.6	0.805	0.135	0.00000451
10	6,000	23.5	46.5	0.799	0.134	0.00000401
11	6,600	23.8	46.5	0.809	0.136	0.00000369
12	7,200	23.5	46.4	0.798	0.134	0.00000333
13	7,800	23	46.4	0.783	0.132	0.00000301
14	8,400	22.5	46.5	0.766	0.129	0.00000273
15	9,000	22.2	46.5	0.754	0.127	0.00000251

3.4.3. Third Reading

Table 13: Reading 3 at 6500 Gauss

Meas. Pts.	Time	Viscosity	Temperature	Shear Stress	Torque	Relaxation Modulus
	[s]	[cP]	[°C]	[Pa]	[mNm]	[Pa]
1	600	26.6	46.6	0.903	0.152	0.0000588
2	1,200	22.6	46.6	0.769	0.129	0.0000215
3	1,800	21.8	46.6	0.742	0.125	0.0000132
4	2,400	21.4	46.5	0.729	0.122	0.00000952
5	3,000	21.3	46.5	0.723	0.121	0.00000745
6	3,600	19.9	46.5	0.678	0.114	0.00000578
7	4,200	19.7	46.6	0.67	0.113	0.00000486
8	4,800	19.8	46.5	0.672	0.113	0.00000425
9	5,400	19.9	46.5	0.677	0.114	0.00000379
10	6,000	20.4	46.5	0.695	0.117	0.00000349
11	6,600	20.9	46.5	0.71	0.119	0.00000324
12	7,200	20.7	46.4	0.704	0.118	0.00000294
13	7,800	20.6	46.4	0.702	0.118	0.0000027
14	8,400	20.6	46.4	0.702	0.118	0.0000025
15	9,000	20.2	46.4	0.685	0.115	0.00000228

3.4.4. Conclusion from Magnetic Treating at 6500 Gauss

Table 14: Compiled Reading at 6500 Gauss

Meas. Pts.	Time	Untreated Crude's Viscosity	Viscosity 1	Viscosity 2	Viscosity 3
	[s]	[cP]	[cP]	[cP]	[cP]
1	600	60.6	26.5	33.6	26.6
2	1,200	61	22	27.5	22.6
3	1,800	62	21	25.2	21.8
4	2,400	62.1	20.7	25.3	21.4
5	3,000	61.5	20.4	25.1	21.3
6	3,600	61.5	20.4	24.6	19.9
7	4,200	61.9	20.4	24.2	19.7
8	4,800	61.3	20.7	24	19.8
9	5,400	60.1	20.6	23.7	19.9
10	6,000	59.2	20.4	23.5	20.4
11	6,600	61.5	20.1	23.8	20.9
12	7,200	60.9	20.3	23.5	20.7
13	7,800	61.1	20.3	23	20.6
14	8,400	61.8	18	22.5	20.6
15	9,000	62.3	18.2	22.2	20.2

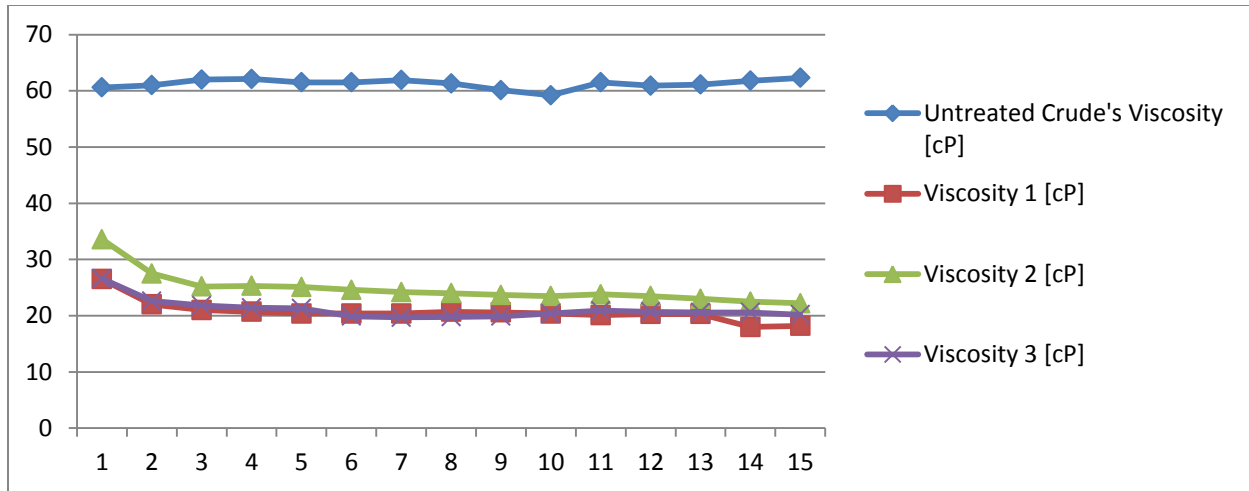


Figure 22: Comparison of Viscosity before treating and after treating at 6500 Gauss Magnetic Field

From above data and graph, rough estimations can be made regarding the viscosity reduction of crude after the magnetic treatment.

$$\% \text{ Viscosity Decline} = \left(\frac{61.2 - 27.2}{61.2} \right) \times 100$$

$$= 55.55 \% \text{ decline in the viscosity}$$

Table 15: Compiled Relaxation Modulus Data at 6500 Gauss Magnetic Field

Meas. Pts.	Time [s]	Relaxation Modulus 1 [Pa]	Relaxation Modulus 2 [Pa]	Relaxation Modulus 3 [Pa]
1	600	0.0000586	0.0000745	0.0000588
2	1,200	0.000021	0.0000262	0.0000215
3	1,800	0.0000127	0.0000153	0.0000132
4	2,400	0.00000918	0.0000113	0.00000952
5	3,000	0.00000717	0.00000879	0.00000745
6	3,600	0.00000591	0.00000712	0.00000578
7	4,200	0.00000504	0.00000598	0.00000486
8	4,800	0.00000445	0.00000516	0.00000425
9	5,400	0.00000392	0.00000451	0.00000379
10	6,000	0.00000348	0.00000401	0.00000349
11	6,600	0.00000311	0.00000369	0.00000324
12	7,200	0.00000288	0.00000333	0.00000294
13	7,800	0.00000265	0.00000301	0.0000027
14	8,400	0.00000219	0.00000273	0.0000025
15	9,000	0.00000206	0.00000251	0.00000228

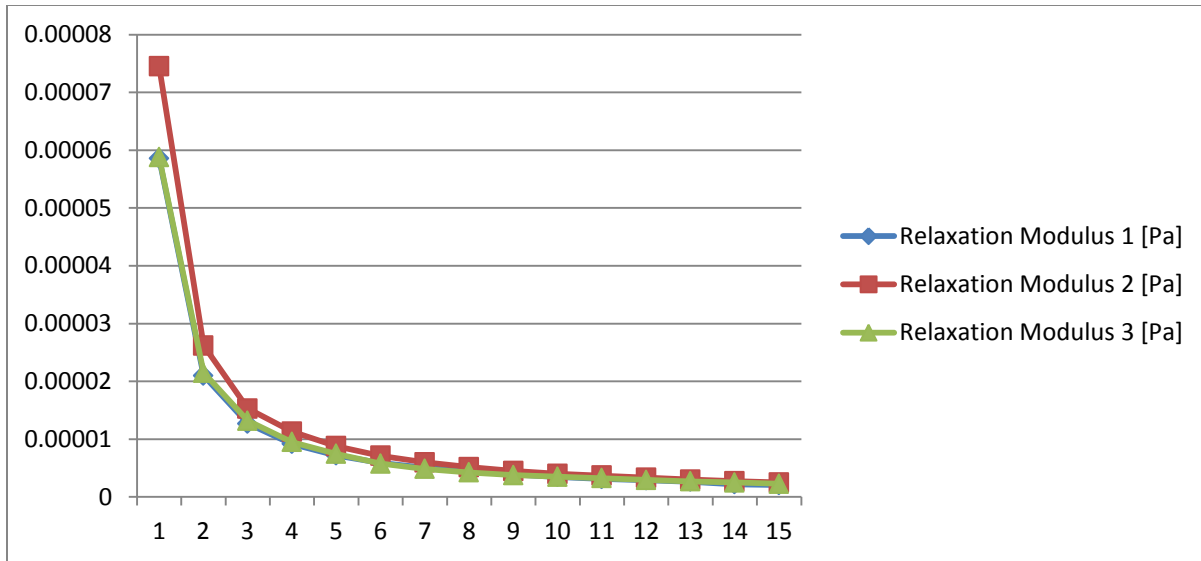


Figure 23: Behavior of Relaxation Modulus of Crude after treating in Magnetic Field of 6500 Gauss

This graph is similar to the previous graph showing the crude as viscoelastic in nature. That means by providing constant shear rate and shear stress, we can decline the bulk modulus exponentially with time.

Moreover, similar trend has been found in the readings of deflection angle between crude and probe when treated at 6500 Gauss Magnetic Field.

Table 16: Compiled Deflection Angle Data at 6500 Gauss Magnetic Field

Meas. Pts.	Time [s]	Deflection Angle 1 [mrad]	Deflection Angle 2 [mrad]	Deflection Angle 3 [mrad]
1	600	1.24E+06	1.24E+06	1.25E+06
2	1,200	2.90E+06	2.90E+06	2.90E+06
3	1,800	4.56E+06	4.56E+06	4.56E+06
4	2,400	6.21E+06	6.21E+06	6.21E+06
5	3,000	7.87E+06	7.87E+06	7.87E+06
6	3,600	9.52E+06	9.52E+06	9.52E+06
7	4,200	1.12E+07	1.12E+07	1.12E+07
8	4,800	1.28E+07	1.28E+07	1.28E+07
9	5,400	1.45E+07	1.45E+07	1.45E+07
10	6,000	1.61E+07	1.61E+07	1.61E+07
11	6,600	1.78E+07	1.78E+07	1.78E+07
12	7,200	1.95E+07	1.95E+07	1.95E+07
13	7,800	2.11E+07	2.11E+07	2.11E+07
14	8,400	2.28E+07	2.28E+07	2.28E+07
15	9,000	2.44E+07	2.44E+07	2.44E+07

Since the value of deflection angle is so large (in terms of 10^6) it can be assumed to be constant up to two decimal places. Therefore it can be found same in some cases that the deflection angle is same.

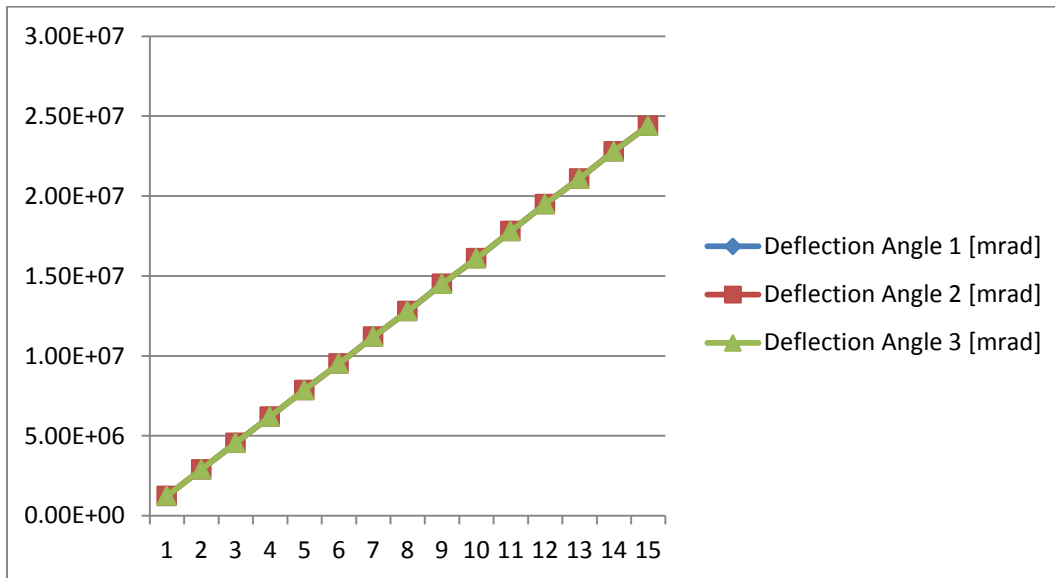


Figure 24: Behavior of Deflection Angle of Crude after treating in Magnetic Field of 6500 Gauss

3.5. Readings at 8000 and 9000 Gauss

We have also performed experiment on elevated magnetic field that is at 8000 Gauss and 9000 Gauss three times to ensure the consistency in the trend. Instead of increase in the percentage of viscosity drop as compared to crude treated at 7500 Gauss, the value starts declining in 8000 Gauss and more in 9000 Gauss. At 1 Tesla again the crude oil is solidified. The information and graphical details at 8000 Gauss and 9000 Gauss has been shown in the annexure.

3.6. Conclusion from the Static Experiment

This shows that there should be certain threshold magnetic field below up to which viscosity of crude will decline and afterwards again rise up due to aggregation of particles into clusters.

Therefore, the threshold magnitude of field for this particular type of crude is 7500 Gauss. But as we can see from the relative percentage decline that there is hardly difference in the decline rate between 7500, 6800 and 6500 Gauss magnetic field. From economic point of view, 6500 Gauss Magnetic Field is the most feasible installation in pipeline for crude's transportation as it takes less current for generation. Keeping this mind, we have conducted viscosity regain time and dynamic test at this magnetic field (i.e. 6500 Gauss).

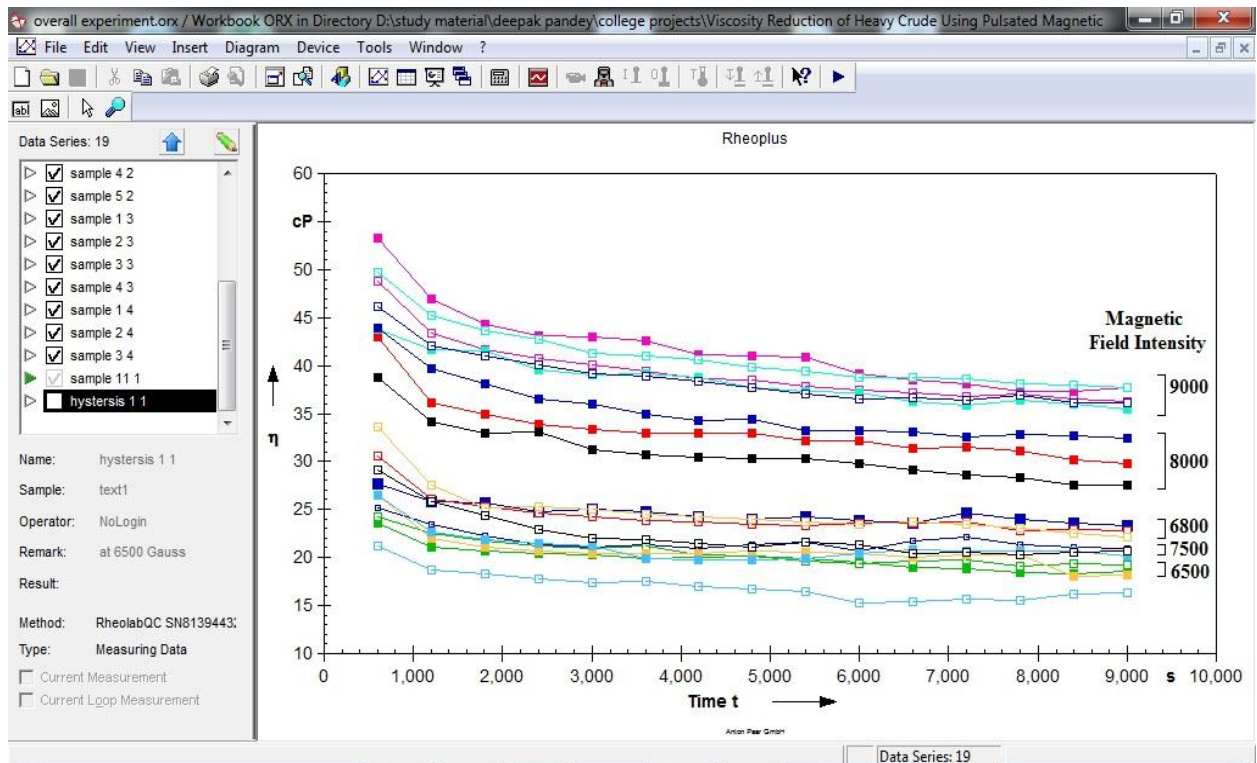


Figure 25: Behavior of Crude's Viscosity at different Magnetic Field Intensity (Courtesy: Snapshot of Anton Parr's Rheoplus Software)

3.7. Viscosity Regain Time Test

The purpose of this test was to ensure when the viscosity of the crude starts rising again, so that it should be again magnetized and could reduce its viscosity. Therefore, we have conducted two tests in the interval of 10 minutes for 7 hours and 8 hours and found that the viscosity is declining maximum up to 8 hours.

3.7.1. Viscosity Regain Test for 7 hours

In this experiment, we have found that viscosity is finally reduced to 18 cP from 24 cP.

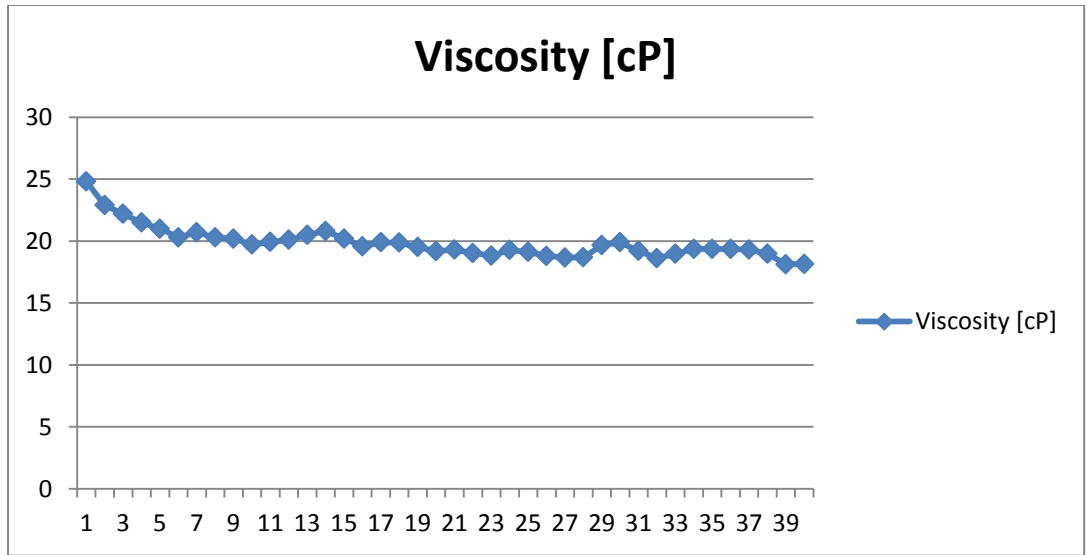


Figure 26: Behavior of Viscosity after 7 hours at 6500 Gauss Magnetic Field

Similarly, there is exponential decline in the Relaxation Modulus of the crude which has been following the same trend as previous graphs at this magnetic field.

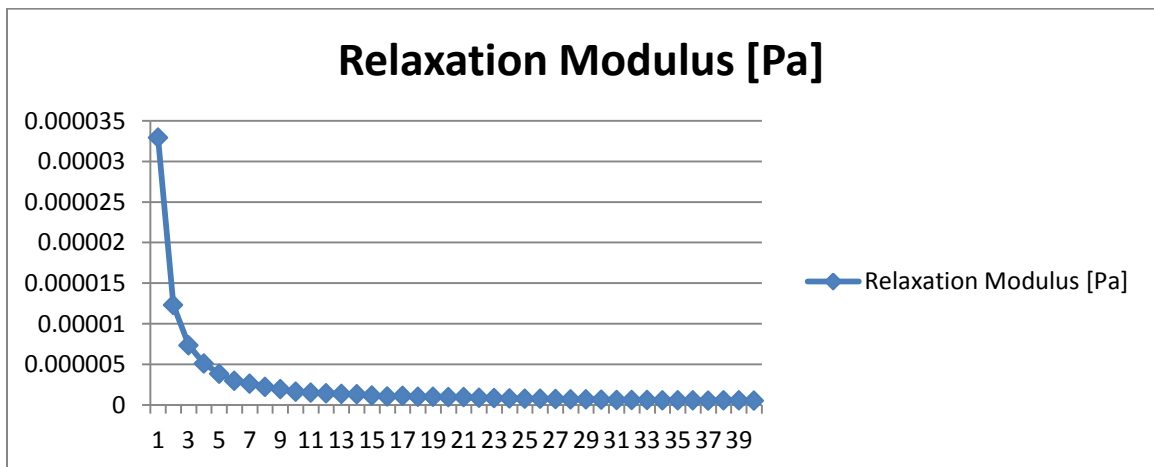


Figure 27: Behavior of Relaxation Modulus after 7 hours at 6500 Gauss Magnetic Field

Meas. Pts.	Time	Viscosity	Temperature	Shear Stress	Torque	Relaxation Modulus	Deflection Angle
	[s]	[cP]	[°C]	[Pa]	[mNm]	[Pa]	[mrad]
1	600	24.8	46.4	0.504	0.0846	0.0000329	1.25E+06
2	1,200	22.9	46.5	0.439	0.0738	0.0000123	2.90E+06
3	1,800	22.2	46.5	0.413	0.0695	0.00000737	4.56E+06
4	2,400	21.5	46.5	0.391	0.0657	0.00000511	6.21E+06
5	3,000	21	46.5	0.374	0.0628	0.00000386	7.87E+06
6	3,600	20.3	46.6	0.349	0.0587	0.00000298	9.52E+06
7	4,200	20.7	46.6	0.363	0.0609	0.00000263	1.12E+07
8	4,800	20.3	46.5	0.352	0.0591	0.00000222	1.28E+07
9	5,400	20.2	46.5	0.346	0.0582	0.00000194	1.45E+07
10	6,000	19.72	46.5	0.33	0.0555	0.00000166	1.61E+07
11	6,600	19.92	46.4	0.337	0.0567	0.00000154	1.78E+07
12	7,200	20.1	46.6	0.343	0.0576	0.00000143	1.95E+07
13	7,800	20.5	46.4	0.356	0.0598	0.00000137	2.11E+07
14	8,400	20.8	46.5	0.368	0.0618	0.00000131	2.28E+07
15	9,000	20.2	46.5	0.347	0.0582	0.00000115	2.44E+07
16	9,600	19.57	46.5	0.326	0.0547	0.00000213	2.61E+07
17	10,200	19.9	46.4	0.336	0.0565	0.00000942	2.77E+07
18	10,800	19.87	46.4	0.336	0.0564	0.00000598	2.94E+07
19	11,400	19.51	46.4	0.323	0.0543	0.00000422	3.10E+07
20	12,000	19.19	46.4	0.313	0.0525	0.00000323	3.27E+07
21	12,600	19.3	46.4	0.316	0.0532	0.00000027	3.44E+07
22	13,200	19.03	46.4	0.307	0.0516	0.00000223	3.60E+07
23	13,800	18.82	46.4	0.3	0.0504	0.00000019	3.77E+07
24	14,400	19.28	46.4	0.315	0.053	0.00000177	3.93E+07
25	15,000	19.12	46.5	0.31	0.0521	0.00000156	4.10E+07
26	15,600	18.8	46.2	0.299	0.0503	0.00000136	4.26E+07
27	16,200	18.67	46.6	0.295	0.0495	0.00000123	4.43E+07
28	16,800	18.69	46.5	0.296	0.0497	0.00000114	4.59E+07
29	17,400	19.66	46.5	0.328	0.0552	0.00000117	4.76E+07
30	18,000	19.9	46.5	0.336	0.0566	0.00000112	4.93E+07
31	18,600	19.2	46.5	0.313	0.0526	9.73E-07	5.09E+07
32	19,200	18.62	46.5	0.293	0.0492	8.57E-07	5.26E+07
33	19,800	18.97	46.5	0.305	0.0513	8.42E-07	5.42E+07
34	20,400	19.37	46.5	0.319	0.0536	8.33E-07	5.59E+07
35	21,000	19.37	46.5	0.318	0.0535	7.90E-07	5.75E+07
36	21,600	19.35	46.5	0.318	0.0534	7.51E-07	5.92E+07
37	22,200	19.32	46.6	0.317	0.0533	7.14E-07	6.08E+07
38	22,800	18.97	46.5	0.305	0.0513	6.57E-07	6.25E+07
39	23,400	18.13	46.5	0.276	0.0465	5.71E-07	6.42E+07
40	24,000	18.15	46.2	0.277	0.0466	5.49E-07	6.58E+07

Table 17: Details of 6 hours 40 minutes Viscosity Regain Test

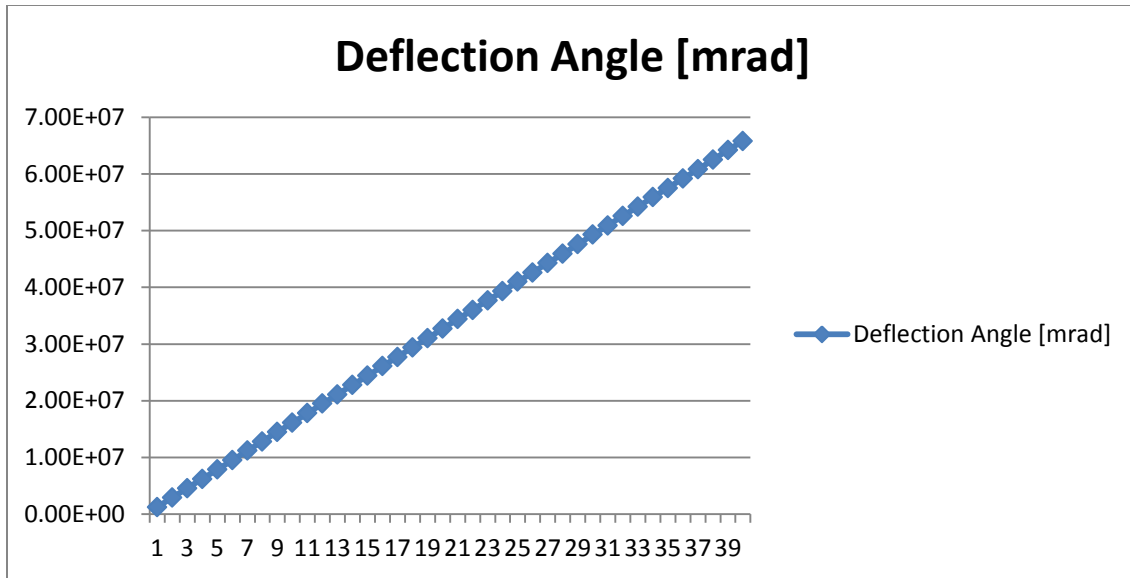


Figure 28: Behavior of Deflection Angle after 7 hours at 6500 Gauss Magnetic Field

The deflection angle is keeping on increasing at same conditions after magnetic treatment and follows similar trend.

3.7.2. Viscosity Regain Test for 8 hours

In this experiment, we have found that viscosity is finally reduced to 14 cP from 24 cP after 7 hours 50 minutes.

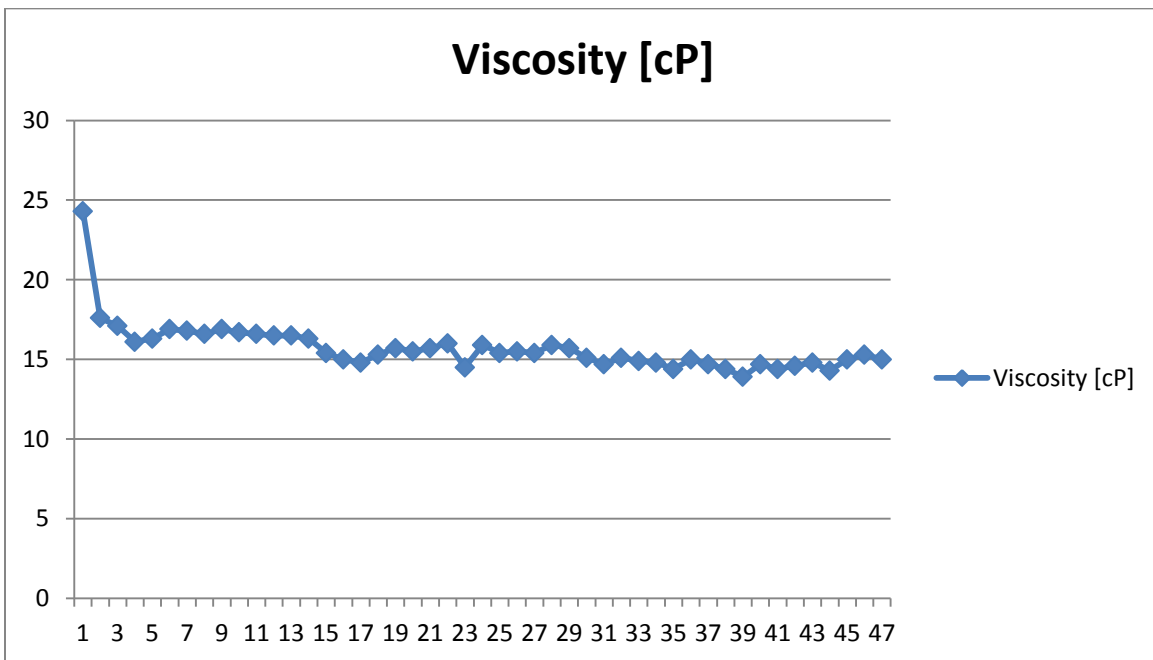


Figure 29: Behavior of Viscosity after 8 hours at 6500 Gauss Magnetic Field

Meas. Pts.	Time	Viscosity	Temperature	Shear Stress	Torque	Relaxation Modulus	Deflection Angle
	[s]	[cP]	[°C]	[Pa]	[mNm]	[Pa]	[mrad]
1	600	24.3	46.5	0.725	0.122	0.0000472	1.25E+06
2	1,200	17.6	46.5	0.597	0.1	0.0000167	2.90E+06
3	1,800	17.1	46.5	0.582	0.0979	0.0000104	4.56E+06
4	2,400	16.1	46.5	0.549	0.0923	0.00000717	6.21E+06
5	3,000	16.3	46.6	0.554	0.0931	0.00000571	7.87E+06
6	3,600	16.9	46.5	0.575	0.0966	0.0000049	9.52E+06
7	4,200	16.8	46.5	0.57	0.0959	0.00000414	1.12E+07
8	4,800	16.6	46.5	0.564	0.0948	0.00000357	1.28E+07
9	5,400	16.9	46.6	0.574	0.0965	0.00000321	1.45E+07
10	6,000	16.7	46.4	0.569	0.0956	0.00000286	1.61E+07
11	6,600	16.6	46.5	0.566	0.0951	0.00000258	1.78E+07
12	7,200	16.5	46.3	0.561	0.0942	0.00000234	1.95E+07
13	7,800	16.5	46.4	0.563	0.0946	0.00000216	2.11E+07
14	8,400	16.3	46.4	0.553	0.0929	0.00000197	2.28E+07
15	9,000	15.4	46.4	0.523	0.0879	0.00000174	2.44E+07
16	9,600	15	46.4	0.509	0.0856	0.00000159	2.61E+07
17	10,200	14.8	46.4	0.502	0.0843	0.00000147	2.77E+07
18	10,800	15.3	46.4	0.519	0.0873	0.00000143	2.94E+07
19	11,400	15.7	46.4	0.534	0.0898	0.0000014	3.10E+07
20	12,000	15.5	46.4	0.526	0.0884	0.00000131	3.27E+07
21	12,600	15.7	46.4	0.534	0.0897	0.00000126	3.44E+07
22	13,200	16	46.4	0.545	0.0915	0.00000123	3.60E+07
23	13,800	14.5	46.4	0.492	0.0826	0.00000106	3.77E+07
24	14,400	15.9	46.4	0.54	0.0907	0.00000111	3.93E+07
25	15,000	15.4	46.4	0.523	0.0878	0.00000103	4.10E+07
26	15,600	15.5	46.4	0.527	0.0885	0.000001	4.26E+07
27	16,200	15.4	46.4	0.524	8.80E-02	9.60E-07	4.43E+07
28	16,800	15.9	46.4	0.541	9.09E-02	9.55E-07	4.59E+07
29	17,400	15.7	46.4	0.534	8.98E-02	9.11E-07	4.76E+07
30	18,000	15.1	46.4	0.513	8.62E-02	8.45E-07	4.93E+07
31	18,600	14.7	46.4	0.501	8.41E-02	7.98E-07	5.09E+07
32	19,200	15.1	46.4	0.512	8.61E-02	7.91E-07	5.26E+07
33	19,800	14.9	46.5	0.507	8.52E-02	7.59E-07	5.42E+07
34	20,400	14.8	46.5	0.505	8.49E-02	7.33E-07	5.59E+07
35	21,000	14.4	46.5	0.49	8.23E-02	6.91E-07	5.75E+07
36	21,600	15	46.5	0.509	8.56E-02	6.98E-07	5.92E+07
37	22,200	14.7	46.5	0.499	8.38E-02	6.65E-07	6.08E+07
38	22,800	14.4	46.5	0.488	8.20E-02	6.34E-07	6.25E+07
39	23,400	13.9	46.5	0.474	7.96E-02	5.99E-07	6.42E+07
40	24,000	14.7	46.5	0.498	8.38E-02	6.15E-07	6.58E+07

41	24,600	14.4	46.5	0.49	8.24E-02	5.89E-07	6.75E+07
42	25,200	14.6	46.5	0.496	8.33E-02	5.82E-07	6.91E+07
43	25,800	14.8	46.5	0.502	8.43E-02	5.75E-07	7.08E+07
44	26,400	14.3	46.5	0.485	8.15E-02	5.44E-07	7.24E+07
45	27,000	15	46.5	0.51	8.57E-02	5.58E-07	7.41E+07
46	27,600	15.3	46.5	0.522	0.0877	5.59E-07	7.57E+07
47	28,200	15	46.5	0.509	0.0855	5.34E-07	7.74E+07

Table 18: Details of 7 hours 50 minutes Viscosity Regain Test

Similarly, there is exponential decline in the Relaxation Modulus of the crude which has been following the same trend as previous graphs at this magnetic field.

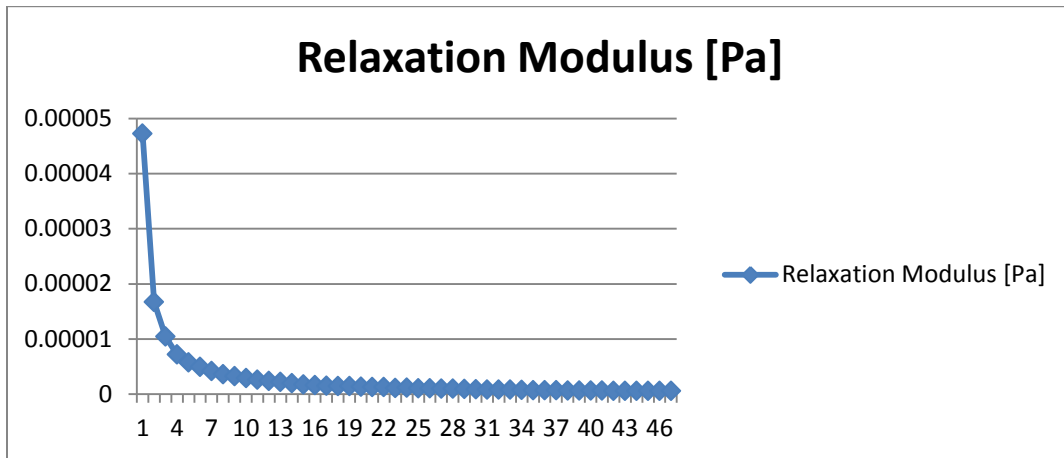


Figure 30: Behavior of Relaxation Modulus after 8 hours at 6500 Gauss Magnetic Field

The deflection angle is keeping on increasing at same conditions after magnetic treatment and follows similar trend.

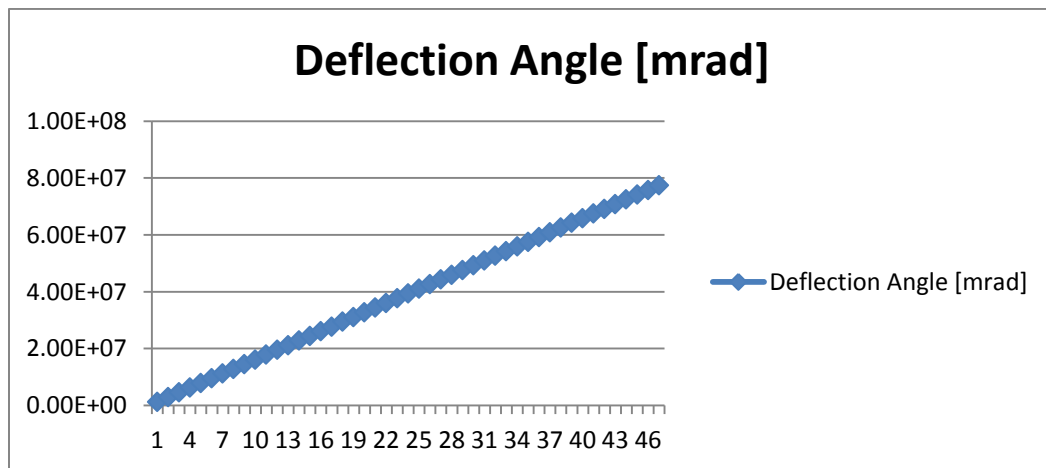


Figure 31: Behavior of Deflection Angle after 8 hours at 6500 Gauss Magnetic Field

The next chapter includes the details of dynamic test conducted at 6500 Gauss field.

Chapter 4: Dynamic Experimental Run

4.1. Design of Experimental Setup for Dynamic Run

The purpose of dynamic run was to ensure whether the effect of magnetic field is valid for stagnant crude or the moving crude or both. Therefore, two sets of designs were proposed to conduct dynamic experiment. In the first layout, crude was to be subjected in a pipeline behave as an electromagnet. One end of the pipeline was attached to the pump and other to the sink. However, in the second layout, a separate apparatus was made containing a PVC pipe was kept between the two poles of magnetic field. These two designs have been discussed below:

4.1.1. Theoretical Design of Apparatus 1

The theoretical design of experimental setup of was consist of a 2 inch ID and 1 meter long pipeline wrapped with a copper coil, a Hall Effect magnetic field sensor probe, a gauss meter and a reciprocating pump. A container was placed at the bottom of the outlet of pump in order to store the crude in it. The purpose of taking mild steel as a material of construction is that most of the crude oil pipelines are made up of mild steel and conducting experiment on it would give us the best result on oil flow behavior during dynamic run.

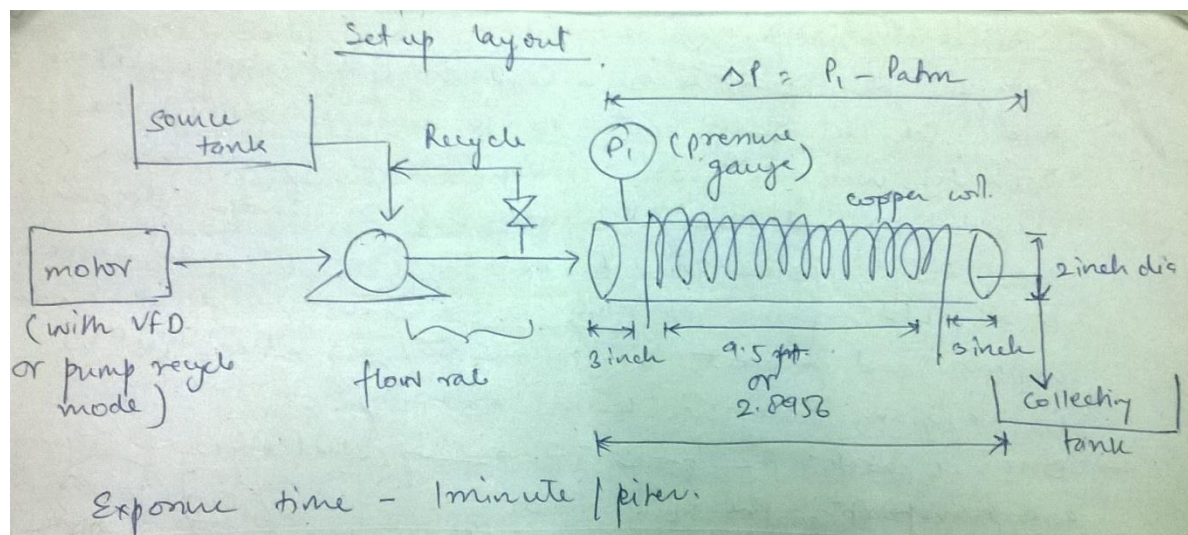


Figure 32: Theoretical Design of Apparatus 1 for Dynamic Run

A aluminum wire of 16 gauge diameter is to be wrapped (1500 turns) in the bobbin made up of same material (i.e. mild steel). An AC supply source direct from the main power line was to be connected with the two ends of copper wire in order to provide current for generation of magnetic field inside the container.

4.1.2. Failure of Apparatus 1 and Rectification of its Limitation



Figure 33: Fabricated Apparatus 1 for Dynamic Run

The Apparatus 1 was producing magnetic field of magnitude 1500 Gauss at the corner and 2000 Gauss at the center when connected to AC supply of 220 V and 27 Amperes current (max permissible value) flowing through it. But fairly high magnetic field ranging from 5000 Gauss (0.5 Tesla) to 1.5 Tesla was required to break the clusters of paraffinic particles and align them in straight line. For increasing the value of field, we can increase the number of turns, but was also heating the pipeline which was not desired.

The reason behind producing low magnetic field was due to the presence of air as a medium inside the container. The magnetic permeability of air is $4\pi \times 10^{-7}$ H/m which is closed to vacuum. Also, the reciprocating pump and gear pump available in the fluid mechanics labs were not able to provide the desired flow rate which was very low (2 liters in one minute). Moreover, the operating temperature of pump was 40 C (as per the vendor). Apart from this the temperature was very difficult to control within the sections of pump due to absence of proper insulating medium

Therefore some new modifications were made in the designs and new apparatus for the experiment was fabricated keeping following things under considerations.

1. Two containers were to install containing water bath at the outlet and crude oil inside the container. An immersion rod of 750 Wattage was to be kept in the water bath for maintaining the constant temperature of the system.
2. Instead of generating the magnetic field in the pipeline, the pipeline section was to be kept between the two poles of an electromagnet.
3. We have also replaced the mild steel pipe with the PVC pipe so that fewer troubles are faced during installations.

4.1.3. Apparatus 2 for Dynamic Test

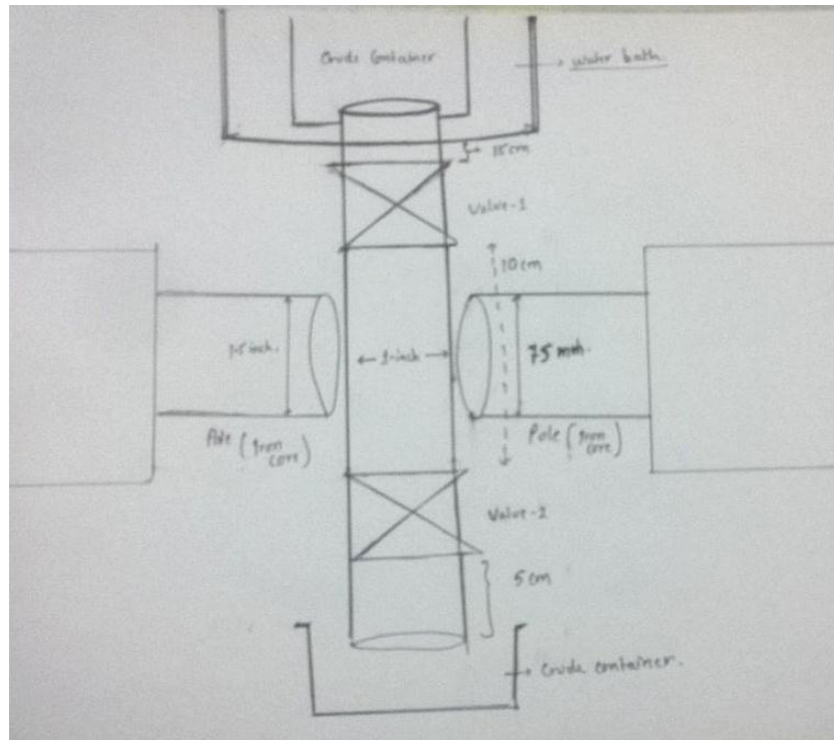


Figure 34: Theoretical Design of Apparatus 2

As discussed in the above section the equipment design included 2 containers, two ball valves in the distance of 10 cm. Since the diameter of poles of electromagnet was 7.5 cm, therefore a clearance of 2.5cm was made from either side of the valves. The diameter of PVC pipe and ball valves were 1.5 inch (outer diameter) and 1.75inches respectively. Insulation from the wool was provided to reduce the drop in the temperature of system. A container was placed at the end of pipeline to store the crude in it.



Figure 35: Apparatus 2

4.2.Procedure of Dynamic Test

1. First of all the crude container and pipeline is washed with the water and then tried to regulate the flow rate of water through the ball valves.
2. Then after the flow rate was achieved, we have performed the experiment on mustard oil at ambient temperature.
3. Then raised the temperature of water bath up to 50° C and allow the crude to stay there for 20 minutes.
4. Then through thermometer the temperature was noted down and then allowed crude to flow freely by keeping valve fully open. Afterwards the temperature of outlet mustard oil was measured and found to be same as at the top i.e. 50° C.
5. Now, both the valves are partially closed in order to achieve the desired flow rate.
6. Once the flow rate was achieved, then again the temperature drop was measured and found to be declined by 7° C.
7. Again the apparatus was washed thoroughly by water and ethanol before performing test on the crude oil sample.
8. Finally the valves are closed partially (less as compared to mustard oil) and then inlet and outlet temperatures were measured at that flow rate and was found to be reduced by 5° C which was less than mustard oil.
9. Once the flow rate was achieved then, the apparatus was installed in between the two poles of electromagnets magnets.
10. As the objective of the experiment is to treat the crude above the pour point, therefore, then crude is heated up to 46° C (treating temperature). The temperature of water bath is maintained few degrees above the treating temperature i.e. at 50° C.
11. Then the crude is treated for 1 minute at different magnetic fields (6500 Gauss, etc.) at 46° C i.e. at treating temperature.
12. Since there is some temperature loss during the magnetic conditioning, therefore the crude is again reheated to 46° C before keeping it into the Rheometer.
13. Finally the crude is placed inside Rheometer to understand the Rheology of crude after magnetic treatment.

The next chapter includes the observations from the dynamic experiment.

Chapter 5: Observations & Outcomes from Dynamic Experiment

5.1.Apparatus Calibration

Before performing experiment, the first step was to calibrate the apparatus in order to reduce the experimental error. Therefore, the desired flow rate of crude oil was calculated which was to be treated at first and tried to obtain same results in the apparatus. Also the temperature drop between the inlet and outlet of the apparatus was checked and kept nearly close to the treating temperature.

5.1.1. Calculation for Desired Flow Rate

Length of Section 1 (between valve 1 and container) = 15 cm

Length of Section 2 (between valve 1 and valve 2) = 10 cm

Length of Section 3 (between valve 2 and outlet) = 5 cm

Diameter of PVC Pipe = 1 inch (0.25 inch thickness)

Diameter of Electromagnetic Poles = 7.5 cm

Clearance = 2 cm

Treating time = 50 seconds

Section of apparatus to be treated in the magnetic field = Section 2

Therefore, the desired flow rate in S. I. Unit was

$$\begin{aligned} \text{Volume of Section to be imposed} &= \frac{\pi r^2 l}{4} \\ &= \left(\frac{3.14 \times (2.54)^2 \times 10^{-4} \times 0.1}{4} \right) m^3 \\ &= 50.6465 \times 10^{-6} m^3 \text{ or } 50.64 \text{ ml} \end{aligned}$$

$$\begin{aligned} \text{Desired flow rate} &= \frac{\text{Volume of Crude to be Exposed}}{\text{Time of Exposure}} \\ &= \frac{50.6465}{50} \\ &= 1.024 \frac{\text{ml}}{\text{sec}} \end{aligned}$$

Therefore, the required flow rate to be 1 ml discharged per second.

5.1.2. Temperature Control

The second calibration step was to control the temperature drop of crude from inlet to outlet. In order to do that we have performed a series of procedures that have been discussed below:

1. First of all the crude container and pipeline is washed with the water and then tried to regulate the flow rate of water through the ball valves.
2. Then after the flow rate was achieved, we have performed the experiment on mustard oil at ambient temperature.
3. Then raised the temperature of water bath up to 50° C and allow the crude to stay there for 20 minutes.
4. Then through thermometer the temperature was noted down and then allowed crude to flow freely by keeping valve fully open. Afterwards the temperature of outlet mustard oil was measured and found to be same as at the top i.e. 50° C.
5. Now, both the valves are partially closed in order to achieve the desired flow rate.
6. Once the flow rate was achieved, then again the temperature drop was measured and found to be declined by 7° C.
7. Again the apparatus was washed thoroughly by water and ethanol before performing test on the crude oil sample.
8. Finally the valves are closed partially (less as compared to mustard oil) and then inlet and outlet temperatures were measured at that flow rate and was found to be reduced by 5° C which was less than mustard oil.

5.2. Readings at 6500 Gauss Magnetic Field

5.2.1. Initial Reading

Table 19: Reading 1 at 6500 Gauss

Meas. Pts.	Time	Viscosity	Temperature	Shear Stress	Torque	Relaxation Modulus
	[s]	[cP]	[°C]	[Pa]	[mNm]	[Pa]
1	600	26.5	46.5	0.9	0.151	0.0000586
2	1,200	22	46.5	0.749	0.126	0.000021
3	1,800	21	46.6	0.716	0.12	0.0000127
4	2,400	20.7	46.6	0.702	0.118	0.00000918
5	3,000	20.4	46.6	0.695	0.117	0.00000717
6	3,600	20.4	46.7	0.694	0.117	0.00000591
7	4,200	20.4	46.7	0.694	0.117	0.00000504
8	4,800	20.7	46.7	0.703	0.118	0.00000445
9	5,400	20.6	46.8	0.701	0.118	0.00000392
10	6,000	20.4	46.8	0.693	0.116	0.00000348

5.2.2. Second Reading

Table 20: Reading 2 at 6500 Gauss

Meas. Pts.	Time	Viscosity	Temperature	Shear Stress	Torque	Relaxation Modulus
	[s]	[cP]	[°C]	[Pa]	[mNm]	[Pa]
1	600	26.6	46.6	0.903	0.152	0.0000588
2	1,200	22.6	46.6	0.769	0.129	0.0000215
3	1,800	21.8	46.6	0.742	0.125	0.0000132
4	2,400	21.4	46.5	0.729	0.122	0.00000952
5	3,000	21.3	46.5	0.723	0.121	0.00000745
6	3,600	19.9	46.5	0.678	0.114	0.00000578
7	4,200	19.7	46.6	0.67	0.113	0.00000486
8	4,800	19.8	46.5	0.672	0.113	0.00000425
9	5,400	19.9	46.5	0.677	0.114	0.00000379
10	6,000	20.4	46.5	0.695	0.117	0.00000349
11	6,600	20.9	46.5	0.71	0.119	0.00000324
12	7,200	20.7	46.4	0.704	0.118	0.00000294
13	7,800	20.6	46.4	0.702	0.118	0.0000027
14	8,400	20.6	46.4	0.702	0.118	0.0000025
15	9,000	20.2	46.4	0.685	0.115	0.00000228

5.2.3. Third Reading

Table 21: Reading 3 at 6500 Gauss

Meas. Pts.	Time	Viscosity	Temperature	Shear Stress	Torque	Relaxation Modulus
	[s]	[cP]	[°C]	[Pa]	[mNm]	[Pa]
1	600	29.1	46.5	0.99	0.166	0.0000645
2	1,200	25.8	46.5	0.879	0.148	0.0000246
3	1,800	24.3	46.6	0.827	0.139	0.0000147
4	2,400	22.9	46.7	0.779	0.131	0.0000102
5	3,000	22.1	46.7	0.75	0.126	0.00000773
6	3,600	21.9	46.7	0.744	0.125	0.00000634
7	4,200	21.5	46.7	0.73	0.123	0.0000053
8	4,800	21.1	46.5	0.718	0.121	0.00000454
9	5,400	21.7	46.3	0.737	0.124	0.00000413
10	6,000	21.3	46.2	0.724	0.122	0.00000364

5.2.4. Conclusion from Magnetic Treating at 6500 Gauss

Table 22: Compiled Reading at 6500 Gauss

Meas. Pts.	Time	Untreated Crude's Viscosity	Viscosity 1	Viscosity 2	Viscosity 3
	[s]	[cP]	[cP]	[cP]	[cP]
1	600	60.6	26.5	26.6	29.1
2	1,200	61	22	22.6	25.8
3	1,800	62	21	21.8	24.3
4	2,400	62.1	20.7	21.4	22.9
5	3,000	61.5	20.4	21.3	22.1
6	3,600	61.5	20.4	19.9	21.9
7	4,200	61.9	20.4	19.7	21.5
8	4,800	61.3	20.7	19.8	21.1
9	5,400	60.1	20.6	19.9	21.7
10	6,000	59.2	20.4	20.4	21.3
11	6,600	61.5	20.1	20.9	20.5
12	7,200	60.9	20.3	20.7	20.6
13	7,800	61.1	20.3	20.6	20.3
14	8,400	61.8	20.1	20.6	20.6
15	9,000	62.3	19.9	20.2	20.7

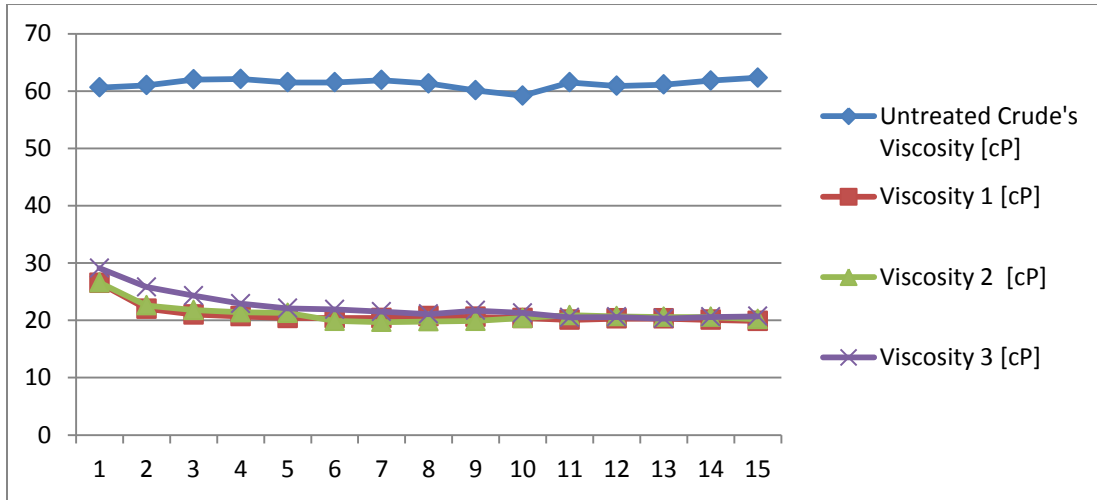


Figure 36: Comparison of Viscosity before treating and after treating at 6500 Gauss Magnetic Field

From above data and graph, rough estimations can be made regarding the viscosity reduction of crude after the magnetic treatment.

$$\% \text{ Viscosity Decline} = \left(\frac{61.2 - 21.2}{61.2} \right) \times 100$$

= 65.83 % decline in the viscosity

This % decline is slightly more than that of same magnetic field reading taken at static conditions. This could happen due to increase in the strength of magnetic field in presence of ferromagnetic substances.

Table 23: Compiled Relaxation Modulus Data at 6500 Gauss Magnetic Field

Meas. Pts.	Time [s]	Relaxation Modulus 1 [Pa]	Relaxation Modulus 2 [Pa]	Relaxation Modulus 3 [Pa]
1	600	0.0000586	0.0000588	0.0000645
2	1,200	0.000021	0.0000215	0.0000246
3	1,800	0.0000127	0.0000132	0.0000147
4	2,400	0.00000918	0.00000952	0.0000102
5	3,000	0.00000717	0.00000745	0.00000773
6	3,600	0.00000591	0.00000578	0.00000634
7	4,200	0.00000504	0.00000486	0.0000053
8	4,800	0.00000445	0.00000425	0.00000454
9	5,400	0.00000392	0.00000379	0.00000413
10	6,000	0.00000348	0.00000349	0.00000364
11	6,600	0.00000311	0.00000324	0.00000317
12	7,200	0.00000288	0.00000294	0.00000292
13	7,800	0.00000265	0.0000027	0.00000265
14	8,400	0.00000219	0.0000025	0.00000249
15	9,000	0.00000206	0.00000228	0.00000234

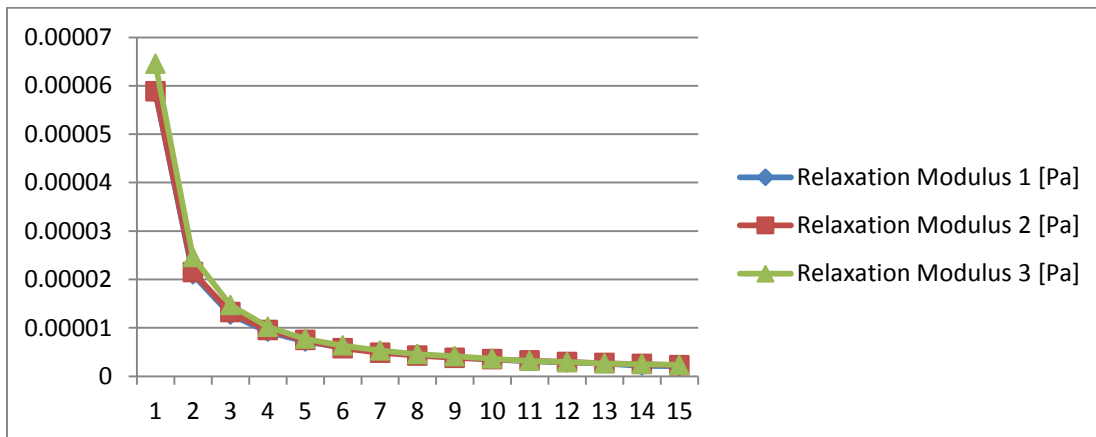


Figure 37: Behavior of Relaxation Modulus of Crude after treating in Magnetic Field of 6500 Gauss

Moreover from above 3 data series we can find the relaxation modulus of crude is decreasing exponentially. The behavior is similar to the static experiment. This graph is similar to the previous graph obtained in static conditions showing the viscoelasticity of crude.

Moreover, similar trend has been found in the readings of deflection angle between crude and probe when treated at 6500 Gauss Magnetic Field. The data and the graph are shown below:

Table 24: Compiled Deflection Angle Data at 6500 Gauss Magnetic Field

Meas. Pts.	Time [s]	Deflection Angle 1 [mrad]	Deflection Angle 3 [mrad]	Deflection Angle 3 [mrad]
1	600	1.24E+06	1.25E+06	1.25E+06
2	1,200	2.90E+06	2.90E+06	2.90E+06
3	1,800	4.56E+06	4.56E+06	4.56E+06
4	2,400	6.21E+06	6.21E+06	6.21E+06
5	3,000	7.87E+06	7.87E+06	7.87E+06
6	3,600	9.52E+06	9.52E+06	9.52E+06
7	4,200	1.12E+07	1.12E+07	1.12E+07
8	4,800	1.28E+07	1.28E+07	1.28E+07
9	5,400	1.45E+07	1.45E+07	1.45E+07
10	6,000	1.61E+07	1.61E+07	1.61E+07
11	6,600	1.78E+07	1.78E+07	1.78E+07
12	7,200	1.95E+07	1.95E+07	1.95E+07
13	7,800	2.11E+07	2.11E+07	2.11E+07
14	8,400	2.28E+07	2.28E+07	2.28E+07
15	9,000	2.44E+07	2.44E+07	2.44E+07

Since the value of deflection angle is so large (in terms of 10^6) it can be assumed to be constant up to two decimal places. Therefore it can be found same in some cases that the deflection angle is same.

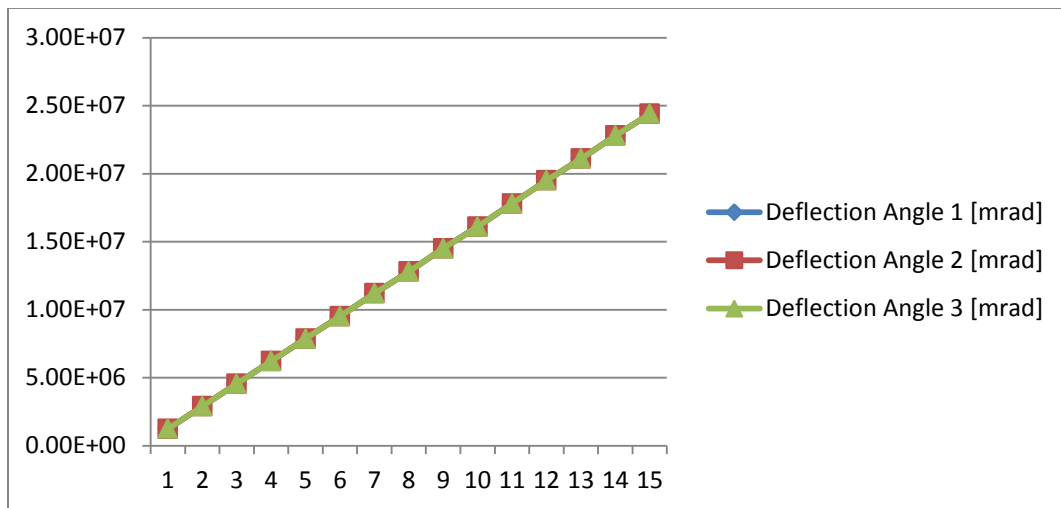


Figure 38: Behavior of Deflection Angle of Crude after treating in Magnetic Field of 6500 Gauss

Hence we can conclude that effect of magnetic field is valid in both static and dynamic conditions. The graph obtained from the software is shown below showing the same trend of viscosity drop which we have obtained in static conditions

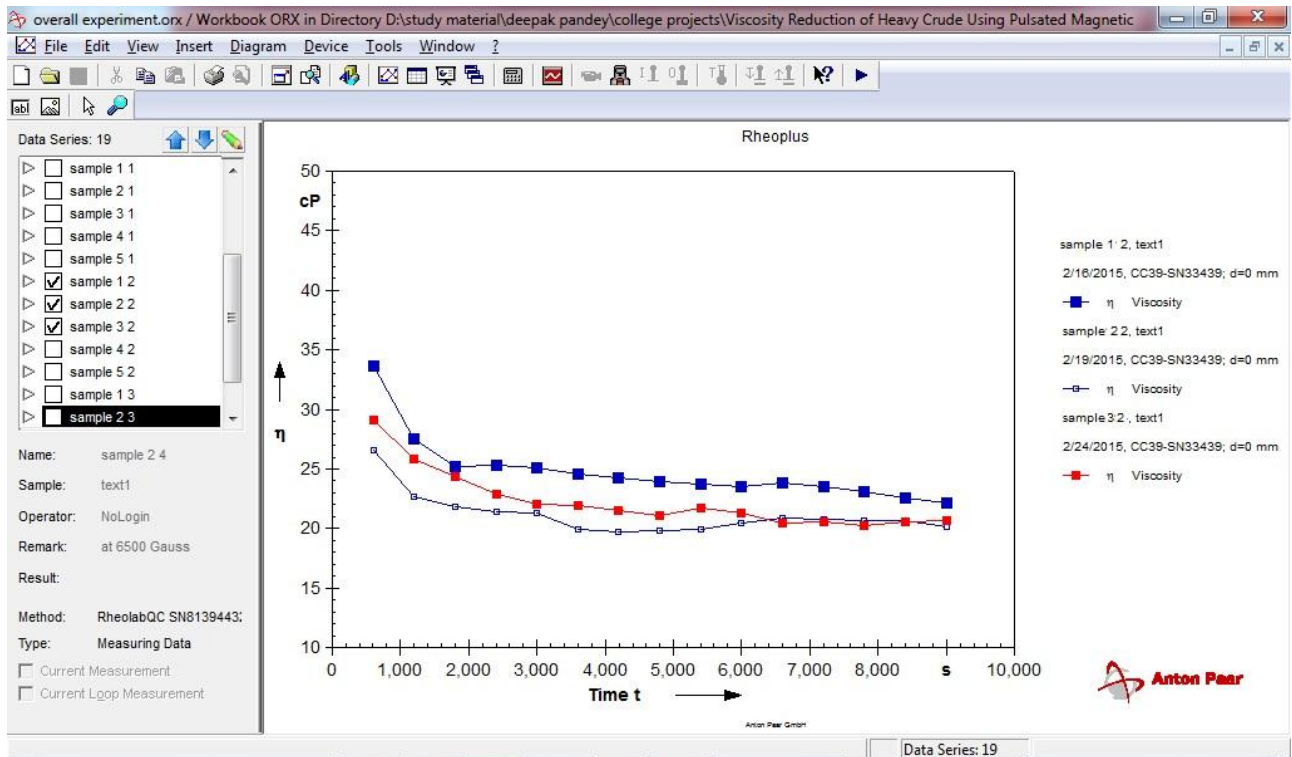


Figure 39: Behavior of Crude's Viscosity at different Magnetic Field Intensity (Courtesy: Snapshot of Anton Parr's Rheoplus Software)

Conclusion & Recommendation

The project was aimed to reduce the viscosity of paraffinic crude with the help of electromagnet. It has been subjected to the magnetic field for short duration and observed that the field breaks the large paraffin clusters into smaller particles due to which there is reduction in the surface tension. As a result, the force of resistance to flow offered by the particles present in the adjacent layers of crude starts declining and causes lowering of viscosity. This experiment was conducted in two conditions i.e. static and dynamic. In static conditions crude is treated in test tube without moving whereas in dynamic run the crude was treated in the flowing conditions.

6.1. Static Experiment Constraints

To check the validity of Tao's Experiment static test was conducted whereas to ensure the validity of magnetic field's effect on moving crude, the dynamic test was conducted. In static test we have found three main effects of magnetic field on crude.

1. The viscosity was brought down (main effect).
2. The bulk modulus was declining exponentially.
3. The contact angle between the crude oil and probe was increasing in ramp manner.

The reason of viscosity decline was clearly expressed in the above statement. As there is reduction in bulk modulus of crude, the outlet pressure starts declining and pressure drop will increase. Due to increase in the pressure drop, the flow rate is maximized. Also on increasing the contact angle between the crude oil and metallic probe, the oil wettability started to cease which would prevent the crude from sticking in the surface of metallic probe.

There were some constraints in the static experiment which are listed below.

1. First of all the calculations that were used for creating the field for the apparatus were not proportional. Moreover due to increase in the air gap the magnetic field lines tend to diverge from each other.
2. When the Wrought Iron Core was fabricated to generate the magnetic field for the experiment, it has been found the limitation in the Hall Effect sensor probe. The probe would sense the field if the direction of field lines is perpendicular to its point of projection. Therefore, we could not measure the intensity of field produced at the center of the Wrought Iron Core.
3. It was supposed to run the static test on metallic surface to understand its behavior, but the current and permeable medium had created obstacles. Therefore, we have taken second model into account to execute our experiment i.e. keeping test tubes between two poles of permanent magnet. It can be assumed that if the effect of magnetic field can be experienced in diamagnetic container (glass test tubes), then it would surely act efficiently when conducted in ferromagnetic container (made up of mild steel, iron, etc.).

4. Major constraint for static experiment was time allotted to perform the experiment in the laboratory which was 9 hours. Therefore, we could not find out the time taken by the crude to regain its original viscosity.

After having good results from the static experiment, we have extended our work in dynamic scale. First of all we have fabricated the instrument and then tried to obtain desired flow rate which we have calculated. Another parameter to be taken into account was the temperature drop. In order to reduce this drop we have conducted the experiment on water, mustard oil and finally on crude. The results obtained in dynamic run was similar to the static run and it shows the repeatability in the experiment.

6.2. Dynamic Experiment Constraints

Like static experiment, there were some constraints present in the dynamic test.

1. Since both the pumps (gear and reciprocating) were not able to maintain very small flow rate therefore new apparatus was fabricated to perform the experiment.
2. There was some time delay in proper treating because the desired flow rate (i.e. 1ml per second) very difficult to achieve.

6.3. Laboratory Constraints

There were limitations in the Laboratory equipment due to which new apparatus were fabricated.

1. As per procedure the test was to be conducted on lower magnetic field as well **but another group was performing an experiment on the same Anton Parr Rheometer.** Therefore, keeping these things under considerations, we have limited our experiment up to only one treating temperature.
2. **The time to perform the experiment was fixed that is 9 hours. Afterwards the readings were aborted as per university rules.** Therefore proper timings were not given to hysteresis test.
3. **Due to absence of metering pumps for low flow rates, many new apparatus were constructed.**
4. **Reciprocating and Gear Pumps could not generate maintain low flow rate.**
5. **The Hall Effect Apparatus was so bulky that it could not be carried from one Lab to another. There was absence of transporting facility in the University for Carrying Equipment from one place to another.**

6.4. Recommendation for future development

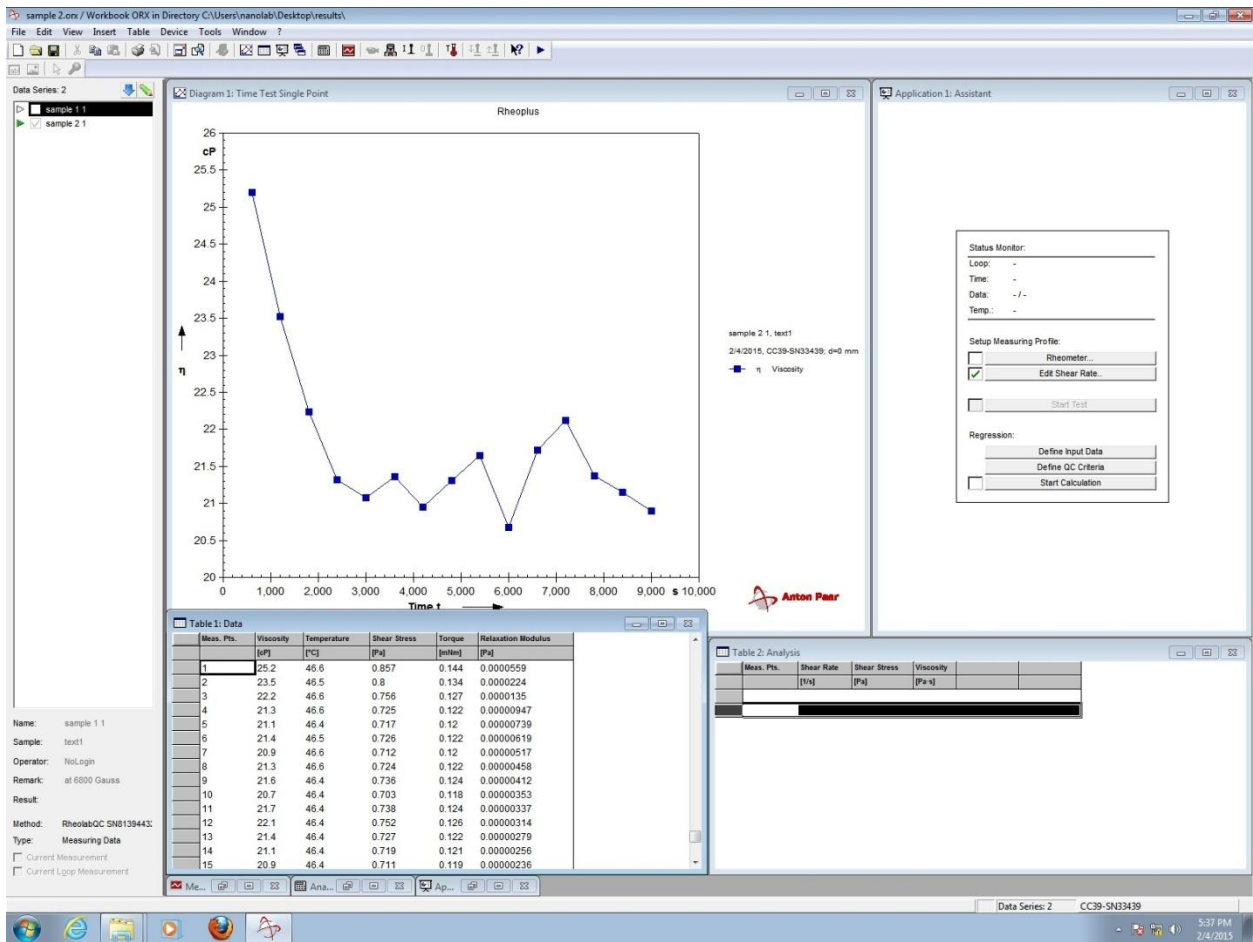
The experiment which was performed showed same results and graphical trends in static and dynamic conditions, but we can recommend few things **which should be implemented in the University for the Success in Major Project and reducing the limitations faced by the students.**

1. **One more set of Anton Parr Rheometer should be brought to the campus** so that ease can be provided to the students who are performing parallel experiments.
2. **Time allotted for the experiments should be increased**
3. **New metering pumps should be purchased for the lower and medium flow rates.**
4. **The existing reciprocating and gear pumps were outdated and hence new pumps to be purchased.**
5. **A facility for transporting bulky apparatus should be purchased so that all the equipments could be assembled at one laboratory.**
6. **An electromagnet should be brought which could generate high magnetic field up to 2 Tesla.**

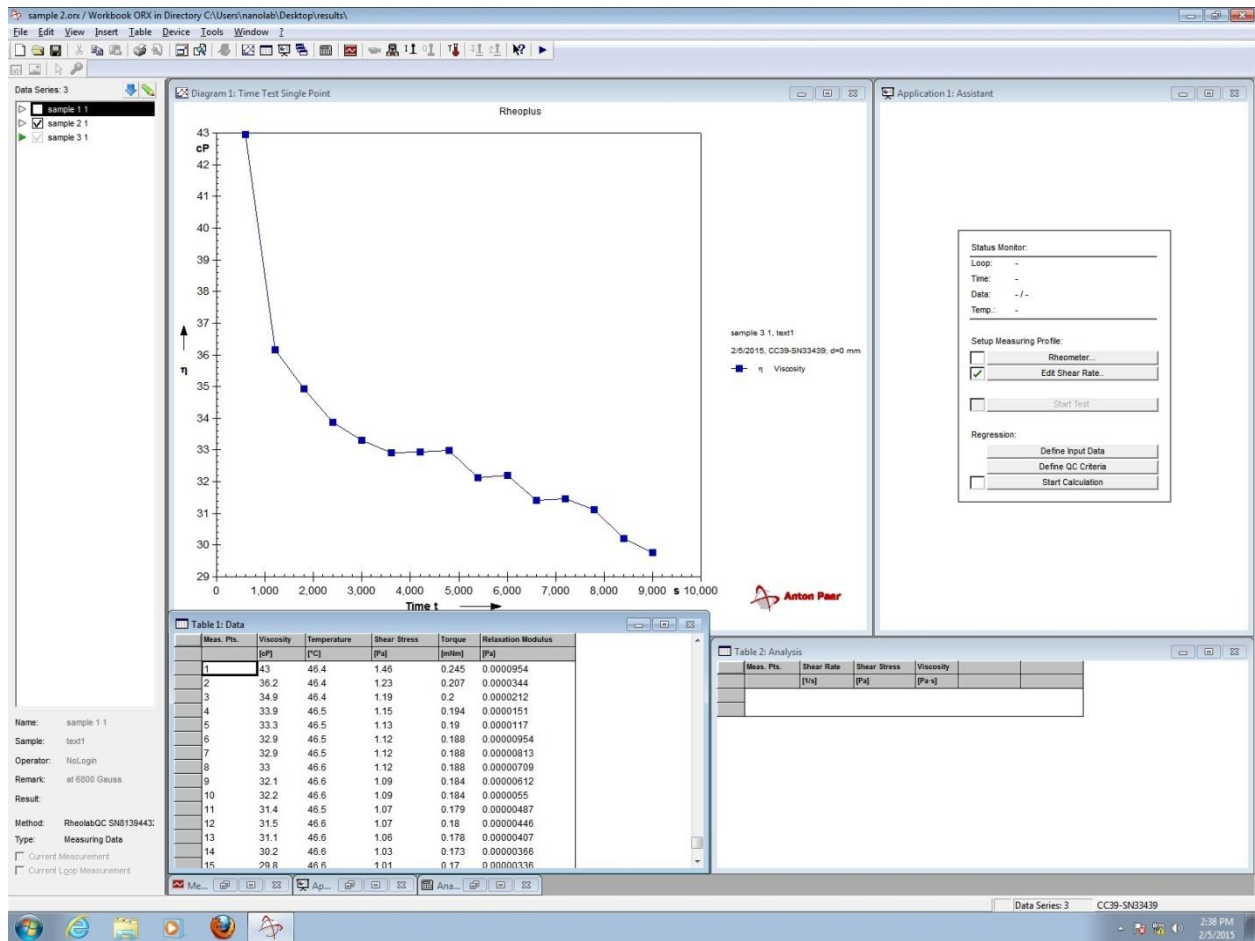
References

- [1] Tao, R., & Xu, X. (2006, September 20). Reducing the Viscosity of Crude Oil by Pulsed Electric or Magnetic Field. *Energy & Fuels* , 20 (5).
- [2] Temple University (2011, June 8). Using magnets to help prevent heart attacks: Magnetic field can reduce blood viscosity, physicist discovers. *ScienceDaily*. Retrieved January 14, 2014, from <http://www.sciencedaily.com/releases/2011/06/110607121523.htm>
- [3] Pandey, D., Singh, A., & Sarkar, A. (2014). Heavy Oil Transportation - Can It Be Made Easier By Magnetism ? *76th EAGE Conference & Exhibition* (p. 2-5). Amsterdam: European Association of Geologists & Engineers.
- [4] (n.d.). Retrieved December 15, 2014, from www.weatherford.com: <http://www.weatherford.com/Products/EngineeredChemistry/ChemicalIntermediates>
- [5] (n.d.). Retrieved December 15, 2014, from www.lubrizol.com: <https://www.lubrizol.com/Energy-and-Water/Oilfield-Chemicals/Production.html>
- [6] (2011, February 28). Retrieved December 15, 2014, from www.oil-additives.evonik.com: <http://oil-additives.evonik.com/sites/dc/Downloadcenter/Evonik/Product/Oil-additives/Publications/Advertisements/Hydrocarbon-Engineering-July-Article.pdf>
- [7] (2010, July 15). Retrieved December 15, 2014, from www.easternsolution.com: <http://www.easternsolution.com/pdf/HP-1540%20Paraffin%20Sticks.pdf>

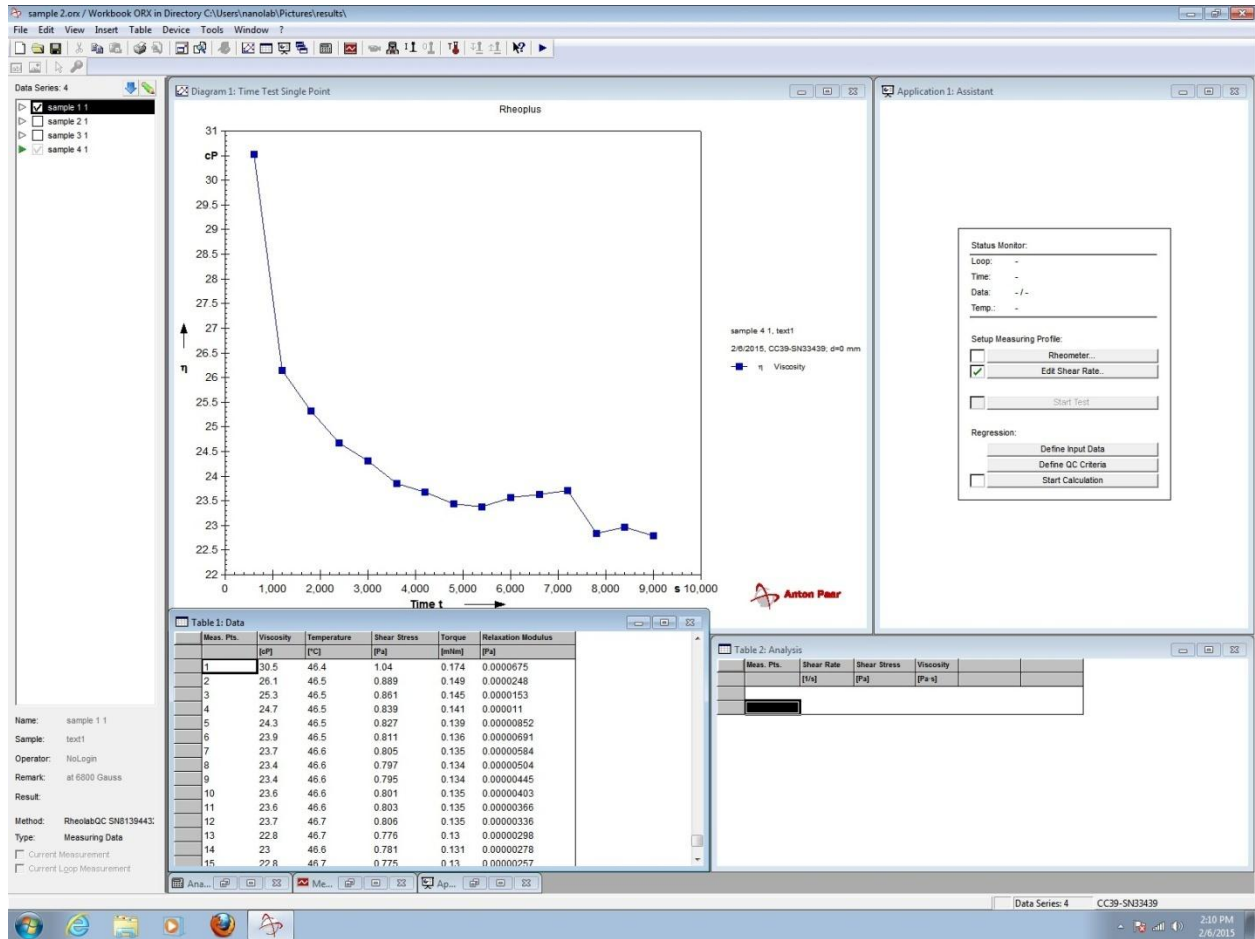
Annexure



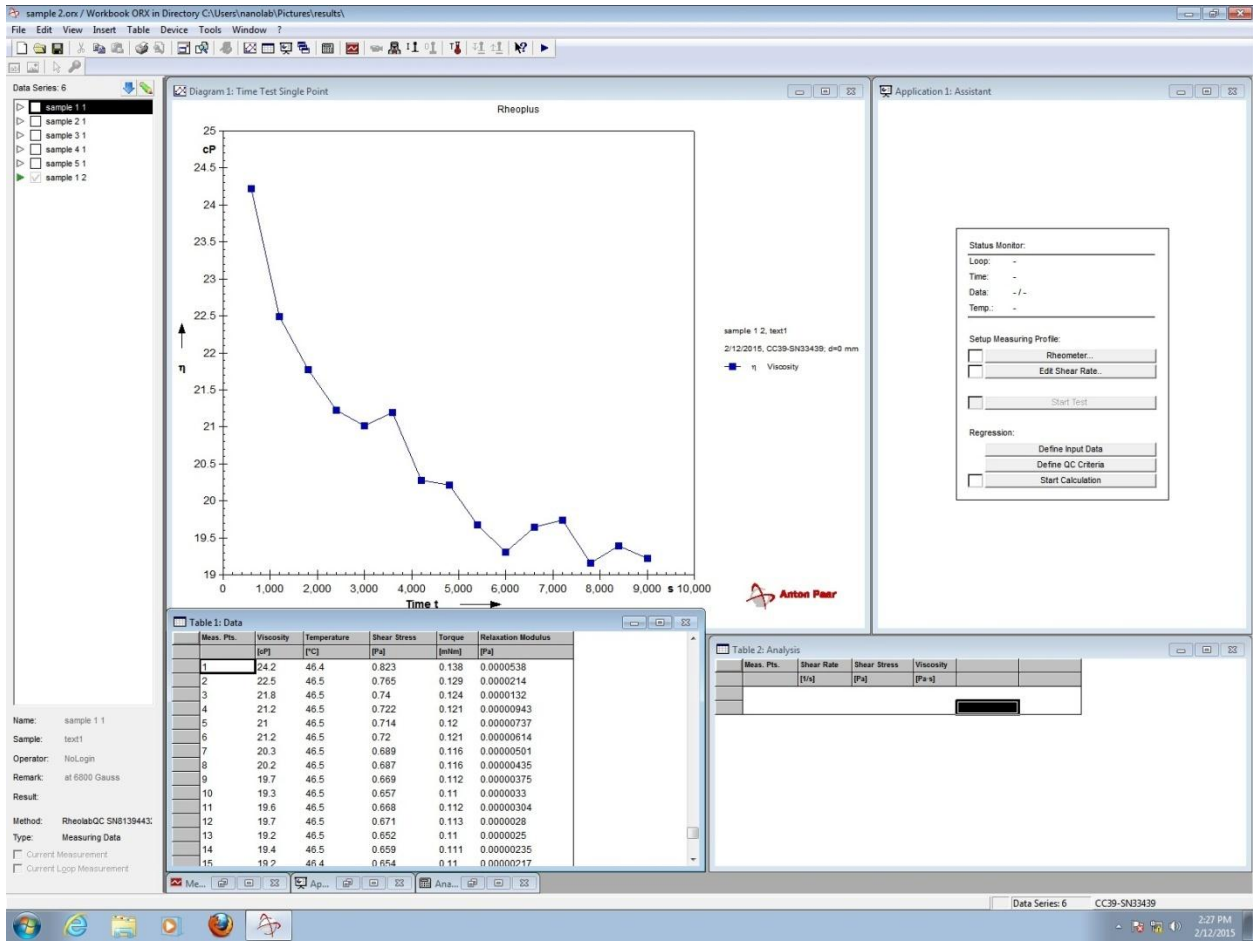
Snapshot 1: Reading 1 at 6800 Gauss Magnetic Field



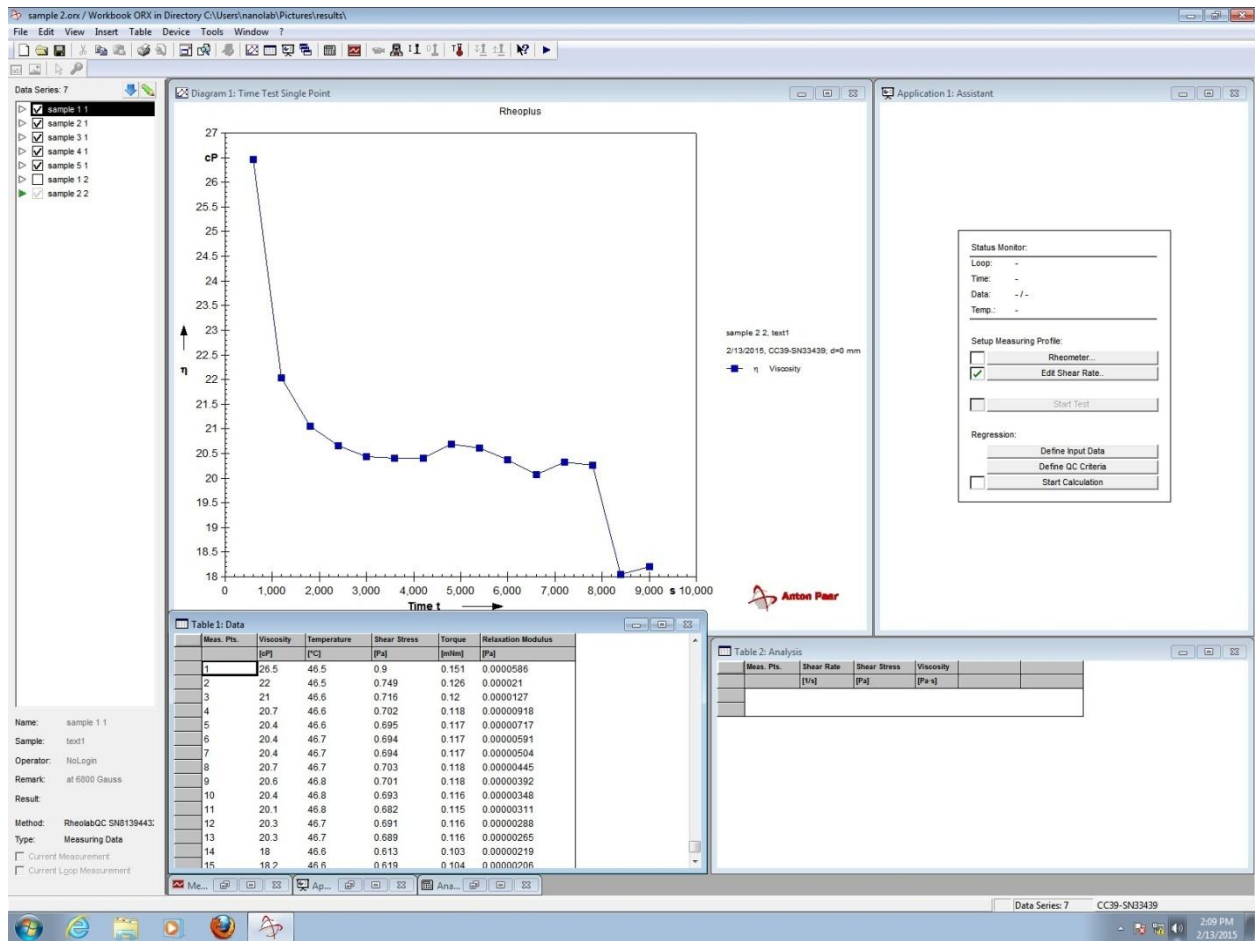
Snapshot 2: Reading 2 at 6800 Gauss Magnetic Field



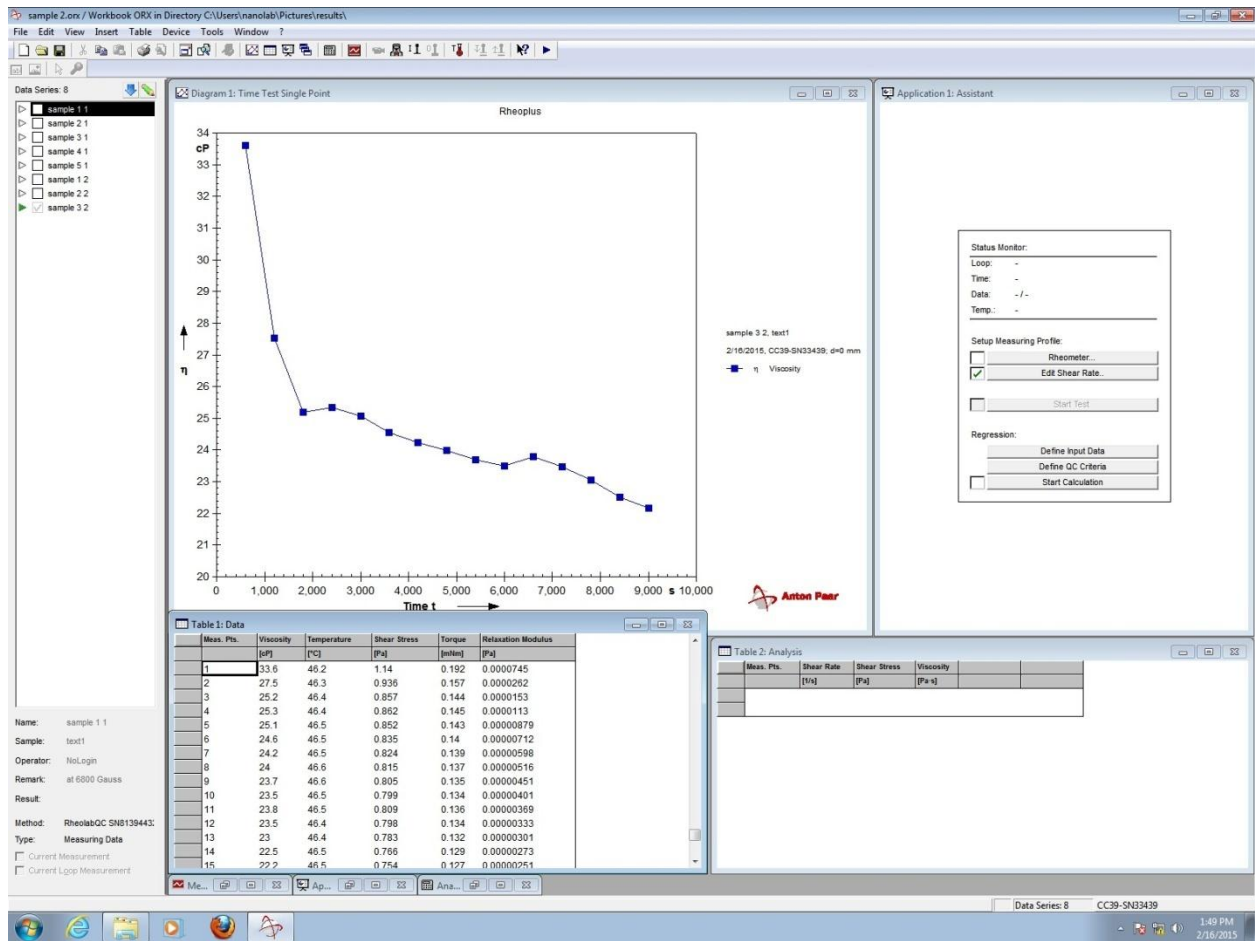
Snapshot 3: Reading 3 at 6800 Gauss Magnetic Field



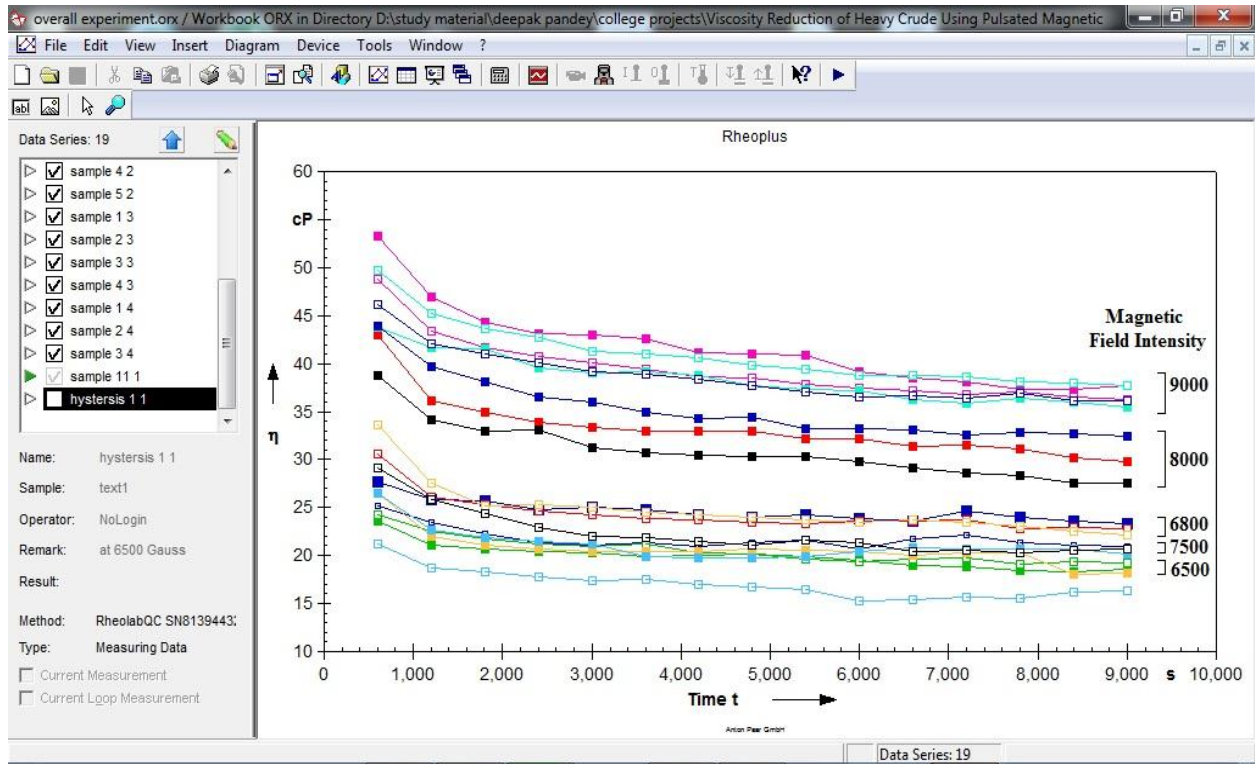
Snapshot 4: Reading 1 6500 Gauss



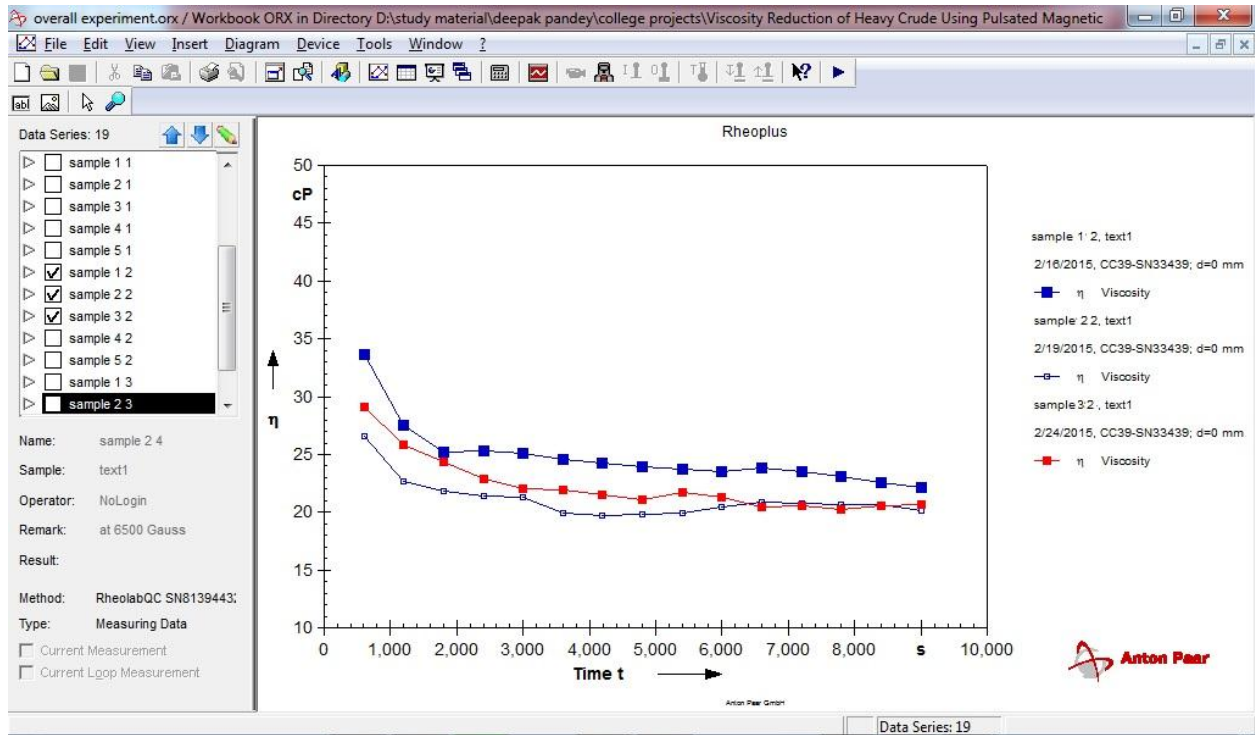
Snapshot 5: Reading 2 at 6500 Gauss Magnetic Field



Snapshot 6: Reading 3 at 6500 Gauss Magnetic Field



Snapshot 7: Compiled Static Readings



Snapshot 8: Compiled Dynamic Reading